

# The Vesosome – A Multicompartment Drug Delivery Vehicle

E.T. Kisak<sup>1</sup> and B. Coldren<sup>1</sup>, C.A Evans<sup>2</sup>, C. Boyer<sup>2</sup> and J.A. Zasadzinski<sup>2\*</sup>

<sup>1</sup>Advanced Encapsulation, 5835 Hollister Ave Ste 209, Santa Barbara, California, 93111, USA

<sup>2</sup>Department of Chemical Engineering, University of California, Santa Barbara, CA 93106, USA

**Abstract:** Assembling structures to divide space controllably and spontaneously into subunits at the nanometer scale is a significant challenge, although one that biology has solved in two distinct ways: prokaryotes and eukaryotes. Prokaryotes have a single compartment delimited by one or more lipid-protein membranes. Eukaryotes have nested-membrane structures that provide internal compartments – such as the cell nucleus and cell organelles in which specialized functions are carried out. We have developed a simple method of creating nested bilayer compartments *in vitro* via the “interdigitated” bilayer phase formed by adding ethanol to a variety of saturated phospholipids. At temperatures below the gel-liquid crystalline transition,  $T_m$ , the interdigitated lipid-ethanol sheets are rigid and flat; when the temperature is raised above  $T_m$ , the sheets become flexible and close on themselves and the surrounding solution to form closed compartments. During this closure, the sheets can entrap other vesicles, biological macromolecules, or colloidal particles. The result is efficient and spontaneous encapsulation without disruption of even fragile materials to form biomimetic nano-environments for possible use in drug delivery, colloidal stabilization, or as microreactors. The vesosome structure can take full advantage of the 40 years of progress in liposome development including steric stabilization, pH loading of drugs, and intrinsic biocompatibility. However, the multiple compartments of the vesosome give better protection to the interior contents in serum, leading to extended release of model compounds in comparison to unilamellar liposomes.

**Key Words :** liposomes, drug delivery, bilayers, lipids, permeability, fusion, serum

## INTRODUCTION

Often, the beneficial and toxic effects of a drug are so delicately balanced that relatively small degrees of selective localization and/or extended exposure are extremely useful. An optimized controlled release delivery system will make possible delivery of both conventional and new, protein- or gene-based drugs with the possibility of targeted specific sites in the body. To be effective, a drug delivery system must (1) have sufficient time in the circulation; (2) be able to be loaded efficiently with sufficient levels of the drug to be delivered; (3) protect the system contents from degradation or premature release, but allow drug release when needed; and (4) passively or actively direct the carrier to specific areas in the body or to specific cell types or tissues. Conventional unilamellar vesicles, or liposomes, have been investigated as drug delivery vehicles for a variety of small molecule drugs since their original discovery in the 1960's [1,2]. Literally thousands of papers have investigated the effects of membrane composition, size, and structure on the therapeutic efficacy of unilamellar liposomes [2-4]. Five liposome-based pharmaceutical products for intravenous injection were approved by the US FDA in the past 6 years, namely DOXIL, Daunosome, Abelcet, Amphotec and Ambisome for systemic delivery of chemotherapeutics

(doxorubicin and daunorubicin) or anti-fungals (amphotericin B). The sales of these products reached \$250 million in 1999, [3] further encouraging research into other long-term drug delivery schemes via liposomes. Cosmeceuticals based on liposomes preceded the pharmaceutical products and liposomes are now a common ingredient in many high-end cosmetic formulations [5].

## TARGETING

The main objectives of using liposomes as drug delivery vehicles is to achieve higher concentrations of drug for extended periods at tumors or inflammation sites, while minimizing the drug exposure to healthy tissues. Selective localization can be obtained by either passive or active targeting. Passive targeting occurs when the physical or chemical properties of the liposomes, together with the microanatomy or chemical environment of the target tissue, enhance drug localization. In the case of cancer chemotherapy, early investigations showed a strong correlation between liposome residence time in blood and uptake by implanted tumors in mice [6]. Increased residence time in the circulation has been largely accomplished by using steric layers of hydrophilic biocompatible polymers, most commonly a polyethylene glycol (PEG) polymer covalently bound to a lipid (PEG-lipids) [7], to hide liposome and nanoparticle carriers from the immune system [8]. Extended circulation times are also associated with making the carriers less than about 250 nm in diameter. Longer circulation times result in repeated passage through

\*Address correspondence to this author at the Department of Chemical Engineering, University of California, Santa Barbara, Santa Barbara, California 93106-5080, USA; 805-893-4769; Fax: 805-893-4731; E-mail: gorilla@engineering.ucsb.edu

the tumor microvasculature and the increased possibility of extravasation from leaky blood vessels at tumor and inflammation sites.

Extravasation at the tumor site is enhanced by the high permeability of tumor microvessels to nanoparticles due to large inter-endothelial fenestrations, discontinuous basement membranes and a high rate of trans-endothelial transport induced by factors secreted by tumor cells such as vascular endothelial growth factor [9]. For liposomes and other carriers less than 250 nm in diameter, the increased permeability of the vasculature surrounding tumors causes the liposomes to selectively build up a larger concentration in the tumor [10,11]. A second factor contributing to the accumulation of liposomes in tumors is the lack of a functional lymphatic drainage in tumors; once in the tumor, the liposomes have no easy way out [11]. The enhanced permeability and retention model, which has been proposed to explain the preferential accumulation of macromolecules in tumors, is also applicable to liposomes [12,13]. Model, animal and human studies have shown an accumulation of liposomes remaining in the tumor interstitial fluid in close proximity to the tumor vessels [10,11]. It is very likely that the success of liposome chemotherapy is due to this passive targeting; however, targeting is not specific to liposomes, but should be common to all nanoparticle drug delivery schemes. Passive targeting also has been observed in infectious or inflammatory pathologies, as substantial liposome localization at the target site has been demonstrated in a variety of models of infection and inflammation [14]. Long-circulation times have been shown to be linearly related to the degree of target localization in inflammation as well [14].

One method of active targeting requires that in addition to reaching the disease site, the carrier must recognize and bind to the specific tissue via antibodies, ligands, etc. The mechanisms and benefits of active targeting are less developed than passive targeting, and as yet, there are no commercially available products that employ active targeting. Recent studies have shown that liposomes targeted against internalizing ligands have higher therapeutic efficacies than those targeted against non-internalizing ligands [15,16]. Non-internalizing liposomes, while showing effective binding to the first line of target cells after extravasation, can obstruct further extravasation of liposomes [3]. Often, the higher the binding affinity to tumor cells, the lower the therapeutic efficiency. This is referred to as the "binding site barrier".

An alternate form of active targeting is controlled destabilization of the membrane by chemical [17] or biological [18] modification of the liposome membrane. It has been observed *in vitro* that doxorubicin and other small, hydrophilic molecule permeability through bilayers is at a maximum near the phase transition temperature of the bilayer, which for dipalmitoylphosphatidylcholine (DPPC) is about 41° C [17]. Addition of small fractions of lyso-phosphatidylcholine (lyso-PC) lowers the temperature of maximum permeability to about 39° C via increased solubility of the lysolipid, which generates defects in the bilayer. Such temperatures can be reached safely by regional hyperthermia. Once the liposomes have been accumulated at the desired site by active or passive means, mild

hyperthermia of the area leads to a fast release of the lysolipid, which in turn causes fast release of the doxorubicin, primarily in the area heated. Other methods of remote targeting use magnetic particles trapped in liposomes and strong external magnetic field to localize the liposomes. [19,20].

## LOADING

Efficient loading of weakly acid or basic drugs has also been well established for conventional unilamellar liposomes using imposed pH gradients [21]. In the case of doxorubicin, additional ions are added to further stabilize the drug (by precipitation or complexation) within the liposome [22]. Loading is based on the observation that the neutral form of drug is often several orders of magnitude more permeable through a lipid membrane than the charged form of the drug (See discussion below). A pH gradient is constructed such that the interior of the liposome is at a lower pH (for weakly basic drugs), usually by incorporating sodium citrate or ammonium sulfate in the liposome interior, followed by neutralizing the exterior solution. In the limit that the charged form of the drug is essentially impermeable, the encapsulated drug concentration inside the liposome,  $[D]_i$ , relative to the external drug concentration  $[D]_o$ , is proportional to the ratio of the proton concentration inside and outside the liposome:

$$\frac{[H^+]_i}{[H^+]_o} = \frac{[D]_i}{[D]_o} \quad (1)$$

Hence, a pH gradient of 3 units leads to a 1000 fold higher concentration of weak base within the liposome as compared to the external environment. For other drugs, like cisplatin, that cannot be loaded via a pH gradient, drug loading can be done at higher temperatures at which the drug solubility may be much higher (~ 8 mg/ml at 65° C vs 2 mg/ml at 37° C). Sometimes, these high interior concentrations can lead to precipitation of certain drugs (doxorubicin in the presence of sulfate is the prime example [22]). It appears, however, that precipitation is often hindered by the small volumes of the liposome and the resulting low probability of finding or creating crystal nucleation sites; intra-liposome solubility can often greatly exceed the bulk solubility at which precipitation occurs [3,23]. This is likely not optimal for controlled release of the drug as the concentration gradient of the drug across the membrane is much higher than is the case for a precipitated drug in the liposome.

## NEW STRUCTURES – MULTIPLE MEMBRANES FOR MULTIPLE TASKS AND MULTIPLE LAYERS OF PROTECTION

Given the tremendous complexities of pharmacokinetics and pharmacodynamics of potential drugs and the immense variety of human disease, it is unlikely that even as versatile structure as the liposome could be the optimal form of drug delivery for all drugs and all conditions. Like the prokaryote

cell, conventional unilamellar liposomes have a single compartment delimited by a single bilayer membrane. This bilayer acts to define the interior space, regulate release of the drug, and protect the bilayer and its contents from attack from the immune system *in vivo*. Essentially all of the literature on liposomes involves modifying the chemical and physical properties of this single membrane to optimize these tasks. This has proven to be difficult, except for a limited number of drugs, namely the doxorubicin (or the chemically similar daunorubicin) in Doxil and the amphotericin B in the anti-fungal preparations.

An alternative to optimizing the chemistry and physics of the single bilayer is to alter the structure of the unilamellar liposome while retaining the lipid membrane as the fundamental structural unit. These new structures include controlled size multilamellar liposomes [24] and large multivesicular liposomes for depot-type drug delivery applications [25,26] and the *vesosome*, Fig. (1) [27]. The multiple membranes and/or multiple compartments dramatically increase the degrees of freedom in optimizing these types of structures for drug delivery or other applications, providing that any added difficulty in assembling the structure is outweighed by these important benefits. In nature, eukaryotes increased their ability to optimize their response to their surroundings by developing multiple compartments, each of which has a distinct bilayer

membrane, usually of quite varied composition and physical structure. Mimicking this natural progression to nested bilayer compartments led to the development of the vesosome, or vesicles deliberately trapped within another vesicle. The vesosome has distinct inner compartments separated from the external membrane; each compartment can encapsulate different materials and have different bilayer compositions. In addition, while it has proven difficult to encapsulate anything larger than molecular solutions within lipid bilayers by conventional vesicle self-assembly, the vesosome construction process lends itself to trapping colloidal particles and biological macromolecules relatively efficiently [27,28]. The nested bilayer compartments of the vesosome provide a degree of freedom for optimization not possible with a single membrane enclosed compartment and a more realistic approximation of higher order biological organization.

For example, encapsulating cationic lipid vesicles [30,31] within a neutral vesicle membrane may provide high drug entrapment efficiency [32], desirable permeability characteristics, or interactions with DNA and other genetic material [30,31], without the associated problems of rapid clearance or flocculation in serum and other biological fluids [2,4,7,8,31-34]. Nested bilayers could significantly extend the encapsulation of both hydrophobic and hydrophilic small molecular weight molecules as each additional bilayer

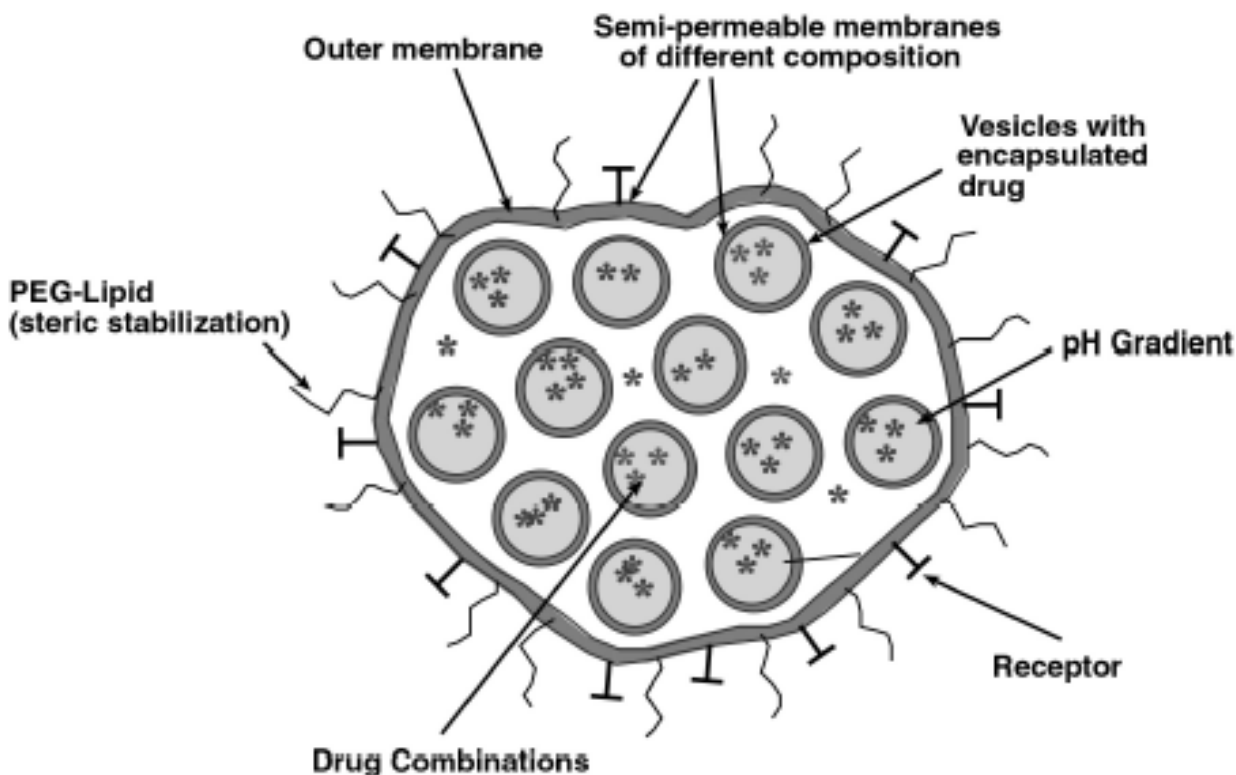


**Fig. (1).** Schematic drawing of the vesosome. The multiple, nested compartments provide a larger number of degrees of freedom to optimize the structure for drug delivery. The nested compartments also provide additional protection against degradation in serum that likely leads to premature release of certain drugs from unilamellar liposomes. The vesosome retains all of the important benefits of conventional liposomes including the possibility of small size and steric stabilization by PEG-lipids for extended circulation times, efficient drug loading by pH gradients, and good biocompatibility.

provides an additional barrier to both permeation and degradation by lipolytic enzymes. Both biocompatibility and stability can be imparted on colloidal particles or emulsion droplets by encapsulation within a bilayer membrane; changes in ionic environment that would lead to flocculation would be interrupted by the bilayer, and the size of the flocs would be limited, minimizing sedimentation. The vesosome structure could be used to deliver a cocktail of antibiotics or antimicrobials to sites at a fixed ratio; such mixtures have been shown to act synergistically when delivered in a single liposome [14]. Such multi-drug formulations may be useful to avoid inducing pathogen resistance to a single drug.

However, it is important to retain the benefits of unilamellar liposomes to drug delivery – namely long circulation times, efficient pH-assisted drug loading, biocompatibility, and formation primarily by either spontaneous or directed self-assembly. As vesosomes are simply liposomes within liposomes, it should be possible to directly translate the extensive body of research on liposome drug delivery to the vesosome with only minor changes, and perhaps significant major improvements. The vesosome is created by simple self-assembly steps very similar to those used in making conventional unilamellar liposomes [27]. An important question to ask is whether such additional effort in developing new structures will provide a therapeutic benefit over direct injection of the free drug or drug delivery by conventional unilamellar liposomes. The most obvious potential application for the vesosome is for drugs that have already shown increased efficacy by delivery from conventional liposomes, but the improvement is limited by sub-optimal, overly fast release rates. For many of the weakly basic drugs that can be loaded by pH gradients, but that do not form a precipitate, this may be the case.

As an example, ciprofloxacin (cipro), a synthetic bactericidal fluoroquinolone antibiotic with broad spectrum efficacy, is released much more quickly from unilamellar liposomes in serum relative to saline [23,35]. Conventional pH-loaded liposomes can retain essentially all encapsulated ciprofloxacin when stored in buffer for 12 weeks at 21° C and 8 weeks at 37° C [36,37]. Although liposomal cipro has shown increased efficacy due to a prolonged residence of cipro in the blood (free cipro is cleared in minutes), the half-life of release from the liposomes was only 1 hour, yet the liposomes themselves circulated for more than 24 hours [23,37]. A second example is vincristine, a naturally occurring dimeric catharanthus alkaloid that has been used extensively as an antitumor agent since the 1960's. The therapeutic activity of vincristine is dictated by the duration of therapeutic concentrations at the tumor site [36,38,39]. However, vincristine administered to patients by long-term infusion is associated with severe toxicities. Liposomal delivery has offered advantages based on maximizing tumor drug delivery while reducing the accumulation of drug in healthy tissues [36,38,39]. However, conventional liposomes, while offering improved bioavailability, also cannot encapsulate vincristine for sufficient time to give optimal results [36,38,39]. Future work will determine if multiple compartment structures like the vesosome give sufficient enhancement of small drug entrapment to lead to new therapeutics.

## VESOSOME DESIGN AND CONSTRUCTION

### The Basic Requirements for Self-Assembly

Encapsulating vesicles or other chemically or biologically sensitive materials within a bilayer is complicated by the need to protect the interior contents while the exterior membrane is forming, which eliminates most conventional vesicle-forming processes [40]. What is necessary is to have a metastable phase of bilayers that can be opened and closed by processes that do not disrupt other vesicles or compromise biologically or chemically sensitive materials. We take advantage of the ethanol-induced interdigitation of saturated phosphatidylcholines (and related lipids) at low temperature [41,42] that can be reversed by heating to form unilamellar vesicles [43].

Many saturated phospholipids including phosphatidylcholines, phosphatidylglycerols, and phosphatidylserines form an L $\beta$ ' phase in water at temperatures below the main, or chain-melting phase transition temperature, T<sub>m</sub> [44]. In the L $\beta$ ' phase, the crystalline hydrocarbon chains of the lipids are tilted relative to the normal to the bilayer [41,42,44]. The crystalline chains have a smaller projected area per molecule than the hydrated polar groups of the lipids at the bilayer-water interface; hence the chains must tilt to maintain close packing [45]. Above T<sub>m</sub>, the chains melt and take up more area due to the greater conformational disorder of the chains; on average, the chains are normal to the bilayer in the liquid crystalline L $\alpha$  phase [44].

Adding ethanol or other alcohols, glycerol, or propylene glycol to aqueous dispersions of dipalmitoylphosphatidylcholine (DPPC) or other L $\beta$ ' phase dispersions of saturated phospholipids held below T<sub>m</sub> leads to intercalation of these molecules in the lipid polar groups, causing the polar groups to swell and take up even more interfacial area [41,42]. These polar molecules effectively displace water molecules in the polar lipid heads, but do not penetrate deeply into the bilayer [41,42,44]. At some point, increasing the tilt of the hydrocarbon chains is insufficient to allow for efficient hydrocarbon packing while matching the increased interfacial area of the swollen polar groups. Instead of tilting, the hydrocarbon chains of the lipids interdigitate between each other, decreasing the thickness of the bilayer. The amount of ethanol necessary to drive interdigitation is a function of both bilayer curvature and bilayer composition [46]. Interdigitation causes the bilayer to become much more rigid as the two monolayers in the bilayer can no longer glide over each other while bending [43]. The bending rigidity of the bilayer is sufficiently high that the bilayers can no longer form stable, small vesicles; any such structures fuse to form bilayer sheets. The energy of the exposed bilayer edges of the sheets is no longer sufficient to drive the rigid sheets into closed liposome structures [47] as the energy costs of bending the interdigitated bilayers is too great.

We use DPPC, or DPPC mixed with small fractions of polyethylene glycol polymers conjugated to lipids such as dipalmitoylphosphatidylethanolamine (PEG-DPPE), cholesterol (Chol), or dipalmitoylphosphatidylglycerol (DPPG) for the interdigitated sheets as the T<sub>m</sub> for these materials is 41- 43° C [44], and the interdigitated phase is

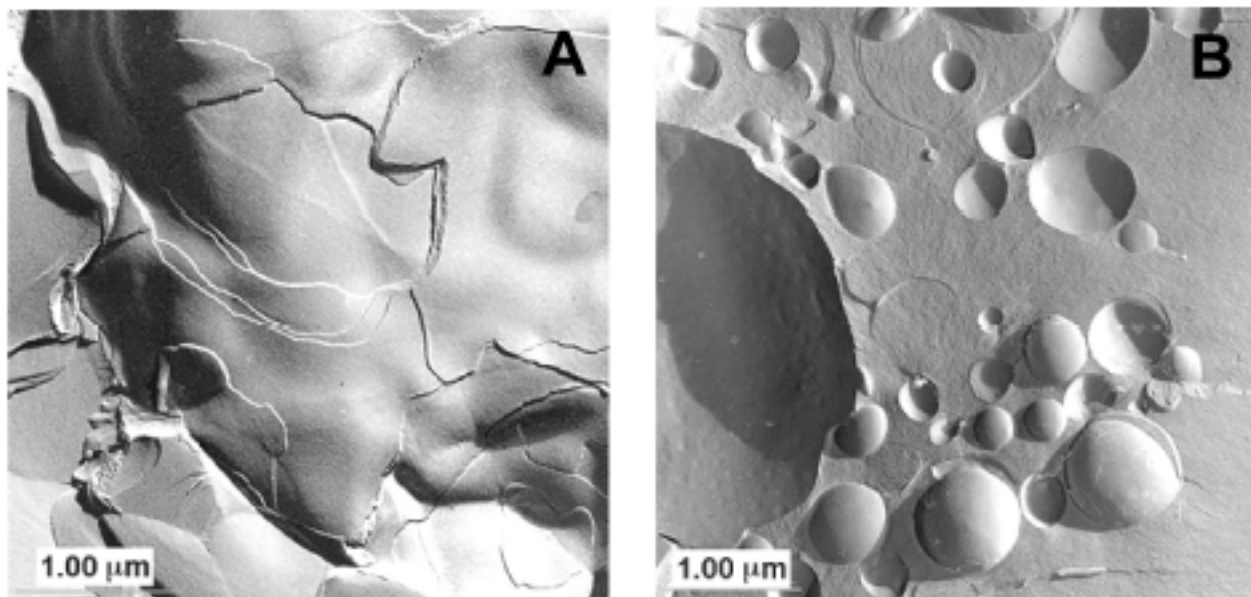


**Fig. (2).** (A) Freeze-fracture TEM image of a stack of interdigitated sheets formed by fusion of 50 nm DPPC vesicles with 3M ethanol. These bilayer sheets are stable even after the excess ethanol was removed from solution as long as the temperature is kept below the melting temperature of the lipid, about 41 C for DPPC.

(B) Unilamellar vesicles form after interdigitated sheets (A) are heated to temperatures above the melting temperature of the lipid used. In this case, the DPPC-3M EtOH sheets are heated to 46C for twenty minutes to form the vesicles. The structures range in size from 0.25 to 3 microns and are usually unilamellar. Prior to preparation for freeze-fracture imaging, the vesicle solution was kept at room temperature for several hours, showing that, once formed, the vesicles are stable.

stable at room temperature, as shown in Fig. (2A). Interdigitated sheets were formed by adding ethanol (typically to a total concentration of 3M) dropwise to 0.5 ml of the 50 nm DPPC vesicle solutions (at concentrations of 25-100 mg lipid/ml) while the solution was stirred. The phase transition is independent of the buffer used; the interdigitated phase forms at almost any salt concentration that would be useful for drug delivery applications. The solution was allowed to sit for two hours to ensure complete interdigitation. The resulting sheets were then washed of excess ethanol by adding 3 ml of buffer followed by centrifuging and removal of supernatant. The sheets were washed three times leaving a residual ethanol concentration less than 0.1M. The interdigitated phase is stable for weeks even after the external ethanol is removed and replaced with water or buffer. However, if the bilayers are heated above  $T_m$ , the hydrocarbon chains of the lipids melt and take up significantly more area; in addition, less ethanol is retained in the polar region [41,42]. The bilayers become less rigid, and the sheets spontaneously close to form unilamellar vesicles, Fig. (2B), [27,43] with an average size of 1.3 microns. For DPPC interdigitated bilayers, we typically heat to 46° C for about 20 minutes [27], which should not degrade most proteins, lipids or other biological molecules. The process can be tailored to the materials being encapsulated – different lipids require different amounts of ethanol to induce interdigitation and have different  $T_m$ 's to induce vesicle reversion. We have also made interdigitated phase sheets from the less expensive surfactants dihexadecylphosphate and dihexadecyldimethylammonium bromide by similar methods [48].

During the reversion from sheets to closed shells, these interdigitated membranes can entrap other vesicles, colloidal particles, biological macromolecules, and perhaps even liquid emulsions. Once vesicles have formed from the sheets, they do not revert to the interdigitated phase even at temperatures below  $T_m$ , Fig. (2B). This encapsulation process is biocompatible and significantly simpler and more efficient than previous methods and does not require specific recognition or other mechanical or chemical processing. The interdigitated phases are also stable to the addition of small fractions of additives – for example, PEG-lipids for steric stabilization or biotin-lipids for specific recognition do not interfere with the phase transition [27].

We have also used the calcium-induced formation of cochleate cylinders by dioleoylphosphatidylserine (DOPS), Fig. (3A) that can be reversed by chelating the calcium [49] to encapsulate vesicles and colloids, Fig. (3B). Essentially any irreversible phase transition between open bilayer sheets and closed shells could be used to make vesosomes [50].

(B) When a 400% excess of EDTA was added to Ca<sup>2+</sup>-induced DOPS cylinders, an assembly of vesicles-within-vesicles formed. The outer envelope of DOPS (white arrow), more than a micron in diameter, encloses smaller vesicles of the same phospholipid (for example, at the black arrows).

### Interior Vesicle Formation

To make the interior vesicles to be loaded into the vesosomes, lipid mixtures (DPPC, DPPC plus cholesterol, distearoylphosphatidylcholine (DSPC) plus cholesterol,

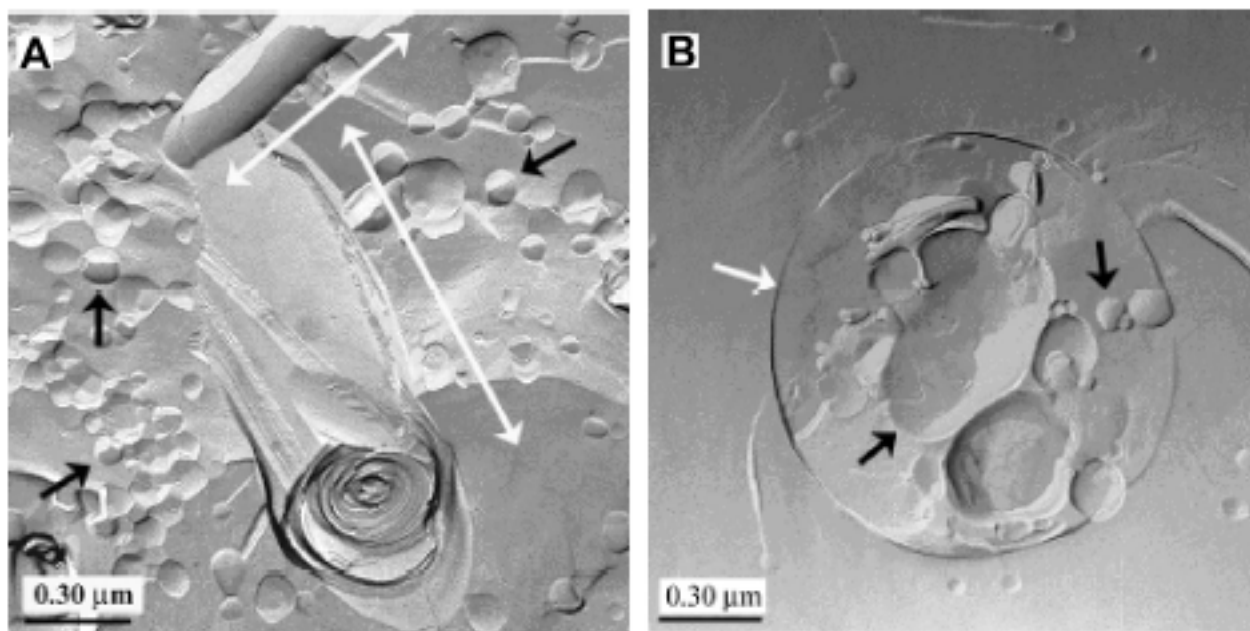


**Fig. (3).** Freeze fracture TEM micrographs of intermediate (a) and final (b) structures in the encapsulation of phospholipid vesicles within an outer envelope of dioleoylphosphatidylserine (DOPS).

(A) Cochleate cylinders of DOPS (parallel to white arrows). The cylinders were formed when 100 nm anionic DOPS vesicles (50 mg lipid/ml, 0.1 mL) fused upon the addition of  $\text{Ca}^{2+}$  (0.1 mL 12 mM  $\text{CaCl}_2$ ). Although some unfused 100 nm vesicles of DOPS are still present (for example, at the black arrows), the cylinders could be isolated by centrifuging or chromatography.

DSPC plus stearylamine and cholesterol, DPPC plus DPPG, egg phosphatidylcholine) were evaporated to dryness in glass ampoules to form thin films of lipids. These lipid films were hydrated with buffer at temperatures above the  $T_m$  of the lipids (45° C for DPPC, 65° C for DSPC). The hydrated lipids were then put through a series of 8 freeze-thaw cycles followed by a series of 8-10 high pressure (approximately 400 psi dry nitrogen) extrusion cycles at 60° C through a Nucleopore filter of pore size 0.05  $\mu\text{m}$  in a Lipex Biomembranes Extruder (Vancouver, Canada). Vesicles for aggregation were prepared as above, but with a 0.16 mol% biotin-X conjugated to dipalmitoylphosphatidylethanolamine (DPPE, Molecular Probes, Eugene, OR) incorporated into the lipid mixture. A stock solution of avidin was prepared in the same buffer at a concentration of 1 mg/ml (1.7  $\times 10^{-5}$  M/l). Aggregation was induced by adding an aliquot of a vesicle stock solution to sufficient avidin solution to form mixtures of the appropriate vesicle concentration at a ratio of receptor to biotin-X DPPE of 1:8.

### Encapsulation

Encapsulation was typically carried out by adding the free vesicles or vesicle aggregates to the pelleted sheets after removing the residual ethanol. The mixture was briefly vortexed and then allowed to heat in a 46° C water bath while being gently stirred. The interdigitated sheets spontaneously closed to form vesosomes, encapsulating the contents of the solution. Separation of vesosomes from excess vesicles was carried out by low speed centrifugation in a desktop centrifuge (~ 2000 rpm). Samples were prepared

by freeze-fracture replication for transmission electron microscopy (TEM) according to standard procedures [27,51].

This process results in the spontaneous encapsulation of vesicles within an external bilayer membrane at approximately the same concentration as the surrounding solution, Fig. (4A). In addition to pure DPPC interdigitated sheets, polymer lipids such as polyethylene glycol lipids (PEG-2000 DPPE, Avanti Polar Lipids) that are commonly used to impart steric stability to vesicles [7], can be incorporated into the interdigitated sheets and used to encapsulate vesicles. Fig. (4B) shows several structures formed from a DPPC/5 mol% 2000 molecular weight PEG-DPPE lipid outer membrane encapsulating 50 nm diameter DSPC/Chol (2:1 mol:mol) vesicles. The interdigitated phase is sufficiently robust that small concentrations of a variety of polymers, ligands, etc. can be incorporated in the encapsulating membrane without disrupting the encapsulation process, thereby making steric stabilization or specific recognition simple to incorporate in the construction process with no additional steps.

The interior vesicles can be made from a variety of lipids as necessary to enhance permeability control, specific interactions, etc. Fig. (5) shows a compartment encapsulating cationic vesicles made from a mixture of 25 % stearylamine, 50% DSPC and 25% cholesterol. The charge or composition of the interior vesicles does not appear to change the encapsulation process. This ability to encapsulate cationic or anionic bilayer vesicles in a neutral lipid bilayer may be important to stabilizing such objects in serum as cationic bilayers are quickly cleared from the bloodstream and can flocculate or clot in serum [32]. This is one of the

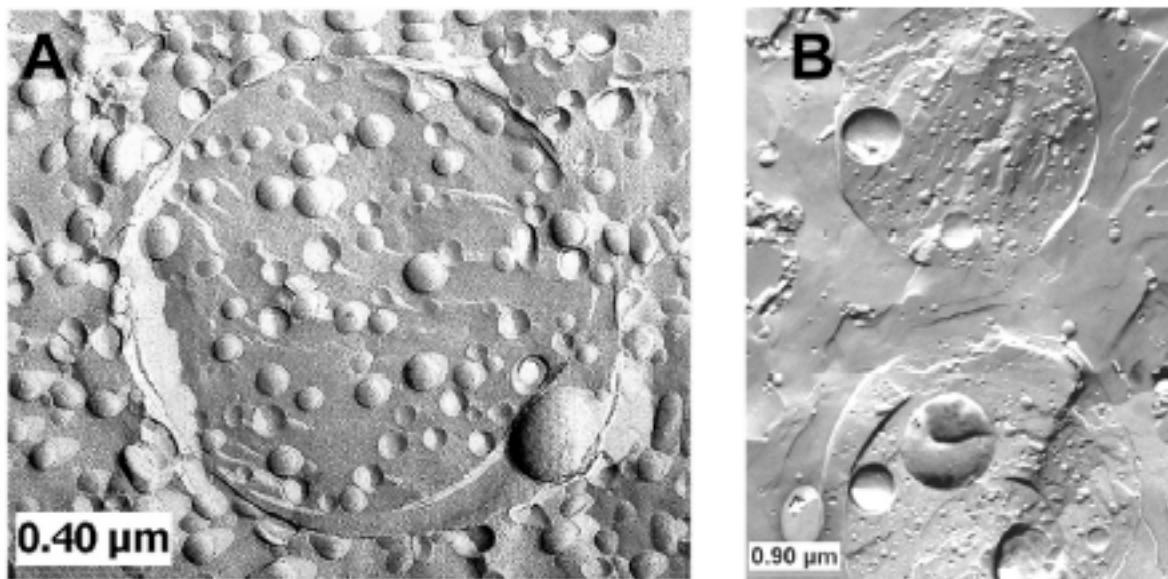


**Fig. (4).** (A) Vesicles were encapsulated in the interdigitated sheets by adding a solution of 50 nm DSPC/Chol (2:1) vesicles (200mg/ml total lipids) to interdigitated DPPC sheets and heating to 46o C. The concentration of DSPC/Chol vesicles inside and outside the interdigitated bilayer is roughly the same.

(B) The interdigitated sheets in this image contain 5 mol% PEG 2000 DPPE lipid that acts to sterically stabilize the outer membrane. The unencapsulated vesicles have been partially removed by centrifugation.

major limitations in using cationic lipid vectors for transfection *in vivo*.

supernatant, once removed from the pelleted fraction, could be recycled to improve the overall efficiency of encapsulation.

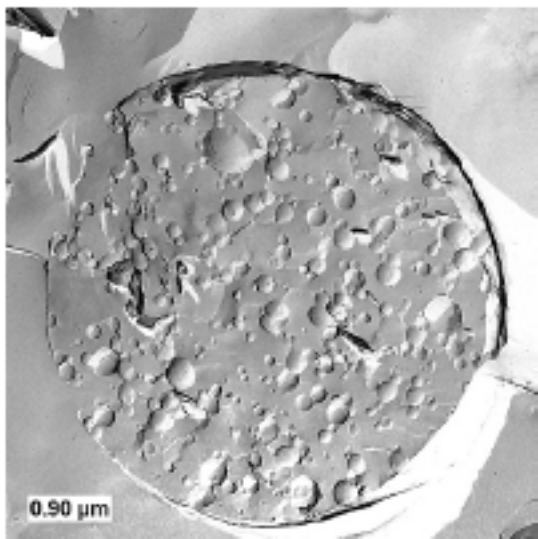


**Fig. (5).** (A) Charged vesicles of 25% stearylamine, 50% DPPC and 25% Chol were encapsulated in DPPC interdigitated sheets. Encapsulating charged vesicles within a neutral membrane should lead to much better stability of these vesicles in a physiological environment.

The unencapsulated vesicles can be separated from the encapsulated materials by gentle centrifugation or even sedimentation if the size difference between the encapsulated particles and unencapsulated vesicles is sufficiently large. Fig. (6) shows pelleted structures with a high density of DSPC/Chol vesicles inside the membranes and virtually no free vesicles outside the membrane after centrifugation. The

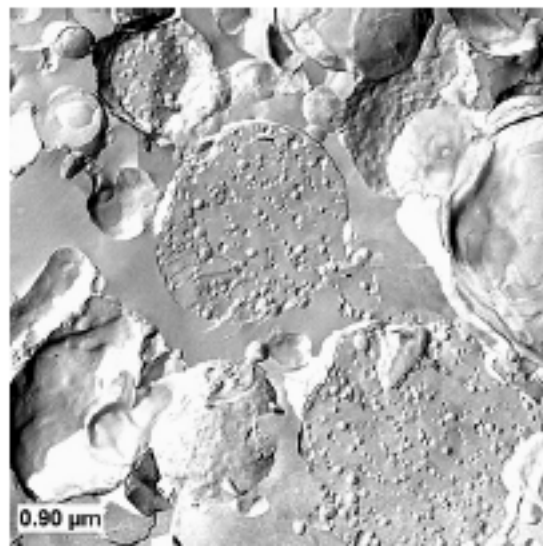


**Fig. (6).** Freeze-fracture TEM image of pelleted vesosomes showing the near complete separation of vesosomes from the unencapsulated 50 nm vesicles. Simple centrifugation or sedimentation is sufficient to do a very efficient separation of vesosomes from unencapsulated vesicles.

### Size Reduction and Control

As discussed in the introduction, to avoid uptake by the immune system and insure long circulation times and passive targeting to tumors or inflamed sites requires that

any drug delivery vehicle for intravenous use should be 250 nm or less [2,3,6,7,11]. Surprisingly, the multicompartiment structure of the vesosome is retained even after size reduction via extrusion through membrane filters [27]. As-formed or centrifuged and separated vesosomes were put through a series of 6-8 high pressure (approximately 400 psi dry nitrogen) extrusion cycles at 60° C through a Nucleopore filter of pore size 0.4  $\mu$ m in a Lipex Biomembranes Extruder (in the same way as the original vesicles were prepared, see previous section) to reduce the vesosome sizes from the as-formed 0.5 – 3 microns to less than 250 nm, Fig. (7). The interior vesicles remain trapped after extrusion even down to an external diameter of about 150 nm. The overall density of the internal vesicles in the vesosome appears to increase after extrusion; this is likely as the surface area to volume ratio increases as the size of the vesosome decreases. At these sizes, the vesosomes should retain the long circulation time and passive targeting of conventional liposomes. Because PEG-lipids can be used for steric stabilization without affecting the interdigitated phase transition Fig. (4B), this reduction in size while retaining the structure is especially significant for extended circulation times. In addition, this final sizing, if performed with sufficiently small filters (0.22 micron), could act as a sterilization step for *in vivo* applications.

### Encapsulation Efficiency

One of the main obstacles to a new structure for drug delivery is the efficiency of formation of the final structure. Vesosomes are made by simple mixing and heating steps and as such, should not be significantly more difficult or costly to make than conventional unilamellar liposomes, if encapsulation can be done efficiently. To determine the efficiency of encapsulation, 50 nm extruded vesicles to be encapsulated were labeled with the fluorescent lipid DPPC-NBD (1-Palmitoyl-2-[6-[(7-nitro-2-1,3-benzoxadiazol]-4-yl)amino]caproyl]-*sn*-Glycero-3-Phospho-choline, Molecular Probes, Eugene, OR) at a 200:1 lipid to dye molar ratio. Various concentrations of labeled vesicles were added to varied concentrations of DPPC interdigitated bilayers followed by heating to form vesosomes as described above. After heating, the solution was diluted 20 fold. A portion of the solution was lysed with the detergent Triton

X-100 and the fluorescent intensity was measured (Imix). The remaining solution was then centrifuged at 2000 rpm for 10 minutes. At this speed, the vesosomes sediment, leaving the unencapsulated vesicles suspended in the supernatant (See Fig. (6); fluorescence measurements of the free vesicles without vesosomes showed that only trace amounts (0- 4%) of these free vesicles sedimented under these conditions). An aliquot of the supernatant was then taken and lysed with Triton X-100 and the fluorescent intensity was measured (Isup). The ratio Isup/Imix gives us the percent vesicles unencapsulated (at these concentrations, the fluorescent intensity is linearly proportional at the concentrations used). Table 1 shows the measured vesicle encapsulation as a function of vesicle and interdigitated sheet concentrations; the efficiencies average ~ 60%. This efficiency is quite high; the maximum volume fraction occupied by identical spheres in random close packing is 63-64%; however, polydisperse spheres or ordering the spheres leads to higher volume fractions. This suggests that the interdigitated sheets encapsulate a significant fraction of the total solution under these conditions.

### Loading Vesosomes by pH Gradient

Efficient loading of weakly basic drugs using imposed pH gradients is another important advantage for liposome use [21], and one that is retained by the vesosome structure. Loading takes advantage of the 3 – 5 orders of magnitude difference in the permeability of membranes to cations vs neutral small molecules. To show this, 50 nm extruded DSPC/Chol (2:1 molar ratio) vesicles were prepared with an interior pH of 4 by making the vesicles in a 300 mM citrate buffer rather than a saline buffer. A sheet concentration of 50 mg/ml DPPC sheets with a vesicle concentration of 25 mg/ml were used to make the vesosomes, which from Table 1, had a vesicle encapsulation efficiency of 62%. Prior to encapsulation, the external pH of the vesicle solution was adjusted to 7.4 using Na<sub>2</sub>CO<sub>3</sub> and prochlorperazine (at a 1:5 drug to lipid ratio) was added to the exterior solution [21], as is typical for conventional liposome loading. Prochlorperazine is a weakly basic drug that can be efficiently loaded using pH gradients in conventional liposomes.

**Table 1.** Measured encapsulation efficiency of vesosome formation using different interdigitated sheet and vesicle concentrations. The interior 50 nm extruded vesicles were made from DSPC/Cholesterol (Chol) (2:1 molar ratio) labeled with 1 part in 200 of the lipid dye DPPC - NBD (1-Palmitoyl-2-[6-[(7-nitro-2-1,3-benzoxadiazol]-4-yl)amino]caproyl]-*sn*-glycero-3-phosphocholine). There is an increase in vesicle encapsulation with increased sheet concentration and a decrease in vesicle encapsulation with an increase in vesicle concentration.

Sheet Concentration	Vesicle Concentration	Encapsulation Efficiency
25 mg/ml DPPC	25mg/ml DSPC/Chol	56%
<b>50 mg/ml DPPC</b>	<b>25 mg/ml DSPC/Chol</b>	<b>62%</b>
75 mg/ml DPPC	25 mg/ml DSPC/Chol	63%
67 mg/ml DPPC	17 mg/ml DSPC/Chol	70%
67 mg/ml DPPC	33 mg/ml DSPC/Chol	66%
<b>67 mg/ml DPPC</b>	<b>50 mg/ml DSPC/Chol</b>	<b>63%</b>

Loading was carried out before encapsulation by heating the citrate-loaded vesicles in the prochlorperazine solution to about 60° C for one hour [21] (liposome loading efficiencies of ~ 100% were seen under these conditions). The increased temperature increases the permeability of the bilayer to neutral prochlorperazine and allows the drug to rapidly equilibrate with the interior citrate and accumulate according to Eqn. 1. The prochlorperazine loaded vesicles were then encapsulated by adding them to interdigitated DPPC sheets at a ratio of 50 mg/ml sheets to 25 mg/ml loaded vesicles and heating as described above. Drug loading efficiency was determined in a similar manner used to measure vesicle encapsulation efficiency, except that Isup was determined by measuring the absorbance of prochlorperazine at 314 nm in the supernatant after centrifugation, following vesicle lysis with SDS (background absorbance from the lipids was subtracted by measuring the absorbance of the supernatant from separated, unloaded vesosomes). Imix was determined from the prochlorperazine absorbance in the uncentrifuged solution following vesicle and vesosome lysis with SDS (Table 2).

**Table 2.** Prochlorperazine was loaded into vesosomes using a 300 mM citrate buffer to generate a pH gradient as for conventional liposome loading. The vesosomes were made from 50 mg/ml DPPC interdigitated sheets and 25 mg/ml DPPC vesicles for which the encapsulation efficiency was 62% (Table 1, bold print). The absorbance of prochlorperazine was used to determine the efficiency of drug loading inside the vesosome for pH loading before, during, and after encapsulation. The efficiency of loading was identical to the efficiency of vesosome formation, indicating that ~ 100% of the drug was loaded into vesosomes.

Drug Loading Procedure	Efficiency
Vesicles Loaded Before Encapsulation	60%
Vesicles Loaded During Encapsulation	63%
Vesicles Loaded After Encapsulation	65%

From these measurements, the fraction of prochlorperazine in the vesosomes was 60%, which is very similar to the fraction of vesicles encapsulated (62% for this ratio, see bold print in Table 1). Hence, virtually all the prochlorperazine was loaded into the vesicle interiors and was retained on vesosome formation.

Loading the interior vesicles can be done equally efficiently during or after encapsulation in the external bilayer. To minimize the number of heating steps, DSPC/Chol (2:1 molar ratio) vesicles prepared with an internal concentration of 300 mM citrate were prepared as previously described. The external pH was adjusted to 7.4 using Na<sub>2</sub>CO<sub>3</sub> and prochlorperazine (at a 1:5 drug to lipid ratio) was added to the exterior solution [21]. In addition, interdigitated DPPC sheets at a ratio of 50 mg/ml sheets to 25 mg/ml vesicles were added to the solution. The solution was then heated to 60° C for one hour to simultaneously load and encapsulate the vesicles into vesosomes. Since the permeability of the neutral prochlorperazine is high, two

barrier membranes should not be appreciably different than one and the charged drug should accumulate in the interior vesicles. The prochlorperazine absorbance was measured before and after centrifugation to determine that the efficiency of prochlorperazine loading in the vesosomes was 63%, essentially the same as that for the vesicles loaded prior to encapsulation. Loading and encapsulating the vesicles simultaneously eliminates one heating step, which may be important for temperature sensitive drugs or to minimize hydrolysis of the lipids.

Drug loading could also be done after the vesosomes were formed. Again, 300 mM citrate buffered DSPC/Chol (2:1 molar ratio) vesicles were formed and the external pH was adjusted to 7.4 using Na<sub>2</sub>CO<sub>3</sub>. These vesicles were then added to interdigitated DPPC sheets at a 50 mg/ml sheets to 25 mg/ml vesicle ratio and encapsulated by heating at 45° C for 20 minutes. Prochlorperazine (at a 1:5 drug to lipid ratio) was added to the vesosome and unencapsulated vesicle solution and heated to 60° C for one hour to load the vesosomes and unencapsulated vesicles with the drug. As before, because the permeability of the neutral prochlorperazine is high, the two barrier membranes of the completed vesosome are not appreciably different than one and the charged drug accumulates in the interior vesicles. The prochlorperazine absorbance was measured before and after centrifugation to determine the efficiency of prochlorperazine loading in the vesosomes was 65%, essentially the same as that for the vesicles loaded prior and during encapsulation. In practice, drug loading would be done after separating the vesosomes from the vesicles to increase the efficiency of loading to nearly 100%. Table 2 shows that the overall drug loading efficiency is comparable to the vesicle encapsulation efficiency of 62% for any pH loading scheme, indicating that essentially 100% of the drug is loaded in the vesosomes. Hence, the vesosome retains the ease of drug loading by pH gradients, which is essential to future use in drug delivery. Vesosomes can be loaded with drug at any convenient step that would maximize the overall efficiency of the process.

### Vesosome Stability

The stability of the vesosome structure against fusion of the interior vesicles is important to retain any advantages inherent to the vesosome. Freeze-fracture images [48] (not shown) showed no apparent difference in vesosomes after 1 month of storage at 4° C. The interior vesicles were well distributed inside the vesosome and there was no indication of the interior vesicles leaking out of or fusing with the encapsulating membrane. To quantify the stability of the interior vesicles against fusion, a pyrene-DPPE fluorescence assay was used. At sufficient pyrene-DPPE concentration in a bilayer (> 2 mole%), pyrene-DPPE excited state dimers (excimers), which have an emission at 475 nm for an excitation at 340 nm, are formed. As the concentration of pyrene-DPPE in the bilayer is diluted by fusion with other bilayers with no pyrene-DPPE, the emission maxima moves to that of the pyrene-DPPE monomer, at about 377 nm [52]. In these experiments, a fraction of the vesicles encapsulated in DPPC vesosomes were labeled with 5 mole% pyrene-labeled DPPE to promote excimer formation, giving rise to a fluorescence emission maxima at 475 nm. If the pyrene-

**Table 3.** Pyrene-DPPE excimer to monomer emission ratio was measured to determine the extent of fusion of interior vesicles with each other and with the external bilayer in vesosomes extruded through 400 nm filters (See Fig. (7)). The percent fusion has a reproducibility of about +/- 3% when measured this way. Addition of 50% charged DHDMA B lipid to the vesicles decreased the amount of fusion due to electrostatic repulsion for both encapsulated and unencapsulated vesicles. Extrusion of the vesosomes did not cause any significant increase in the fusion of the interior vesicles suggesting that they are well protected during the extrusion process.

Composition	Initial Ratio	Initial Fusion	Final Ratio	1 Month Fusion
Extrusion Effect on Stability				
2:1 DSPC/Cholesterol Vesicles	0.160	0% (control)	0.123	20%
Extruded Vesosome	0.156	2.9%	0.144	11%
Unextruded Vesosome	0.158	1.4%	0.137	15.5 %
<b>Charged Interior Vesicles</b>				
50% added DHDMA B	0.0964	0% (control)	0.0938	2.9%
Extruded vesosome	0.0930	3.8%	0.0948	1.8%
Unextruded vesosome	0.0952	1.3%	0.0932	3.5%

DPPE containing vesicles fuse with any unlabeled bilayer, such as the unlabeled encapsulating membrane or the unlabeled population of interior vesicles, the pyrene-DPPE is diluted, fewer excimers are formed, and the emission maximum shifts toward the maxima for monomers. Any fusion is detected as a decrease in the ratio of excimer (475 nm) to monomer (377 nm) emission.

Table 3 shows the results obtained after annealing the labeled vesicles for 15 minutes above the phase transition temperature to assure complete pyrene-DPPE mixing in the labeled DSPC/Chol (2:1) vesicles (the initial 475/377 ratio was taken as the control). Fusion of the vesicles in

vesosomes was compared with a similar concentration of pyrene-labeled vesicles diluted with an unlabeled population of vesicles (1:20 dilution ratio) at similar overall total lipid concentration as those used in the vesosomes. The extent of fusion was measured immediately after vesosome formation (or vesicle mixing) and after one month of storage at 4° C. The decrease in the ratio of the excimer to monomer fluorescence, and hence the rate of fusion, appears to change at a comparable rate for vesicles within the vesosome as compared to free vesicles at the same concentration and composition. For example, the DSPC/cholesterol vesicles showed an apparent 18 – 20% fusion after one month, compared to the 14 - 17% fusion when the same vesicles are

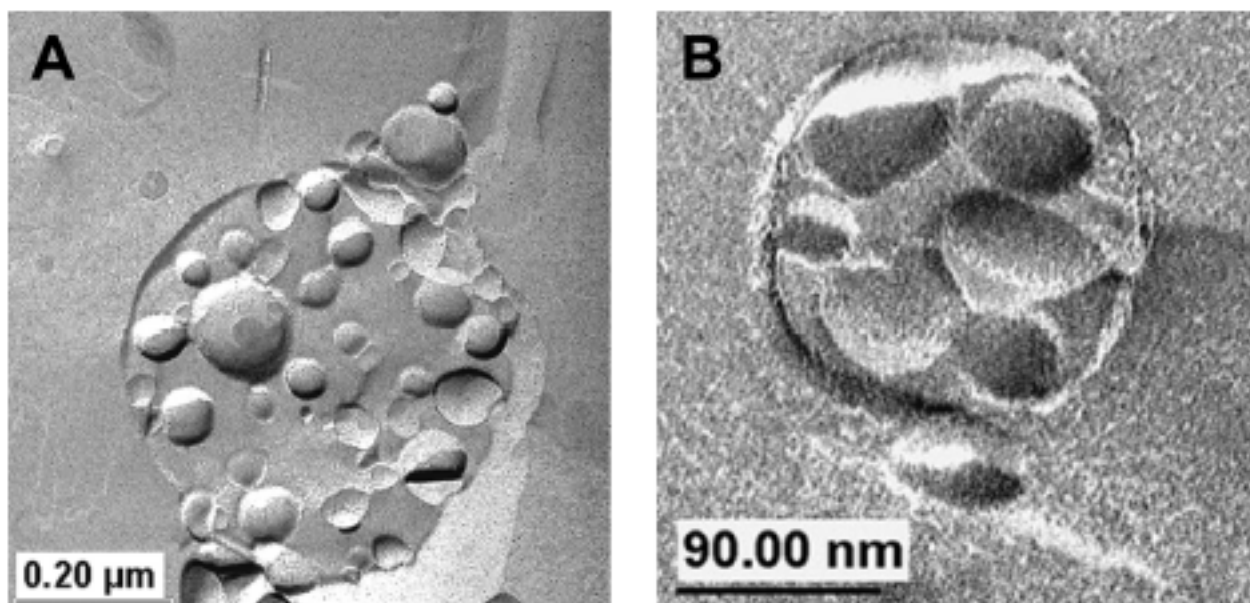


**Fig. (7).** Freeze-fracture TEM images of reduced size vesosomes formed by extruding vesosomes similar to those shown in Fig. (2) Fig. (4) through a 400 nm pore size filter. (A) The vesosome was formed then separated by centrifugation followed by extrusion through a 400 nm filter. Interior vesicles remained encapsulated throughout the process. (B) The vesosome was extruded first then separated. In both cases, the 50 nm interior vesicles were unaffected by the extrusion process and were retained within the outer membrane.

trapped in the vesosome interior. This suggests that the separation of the vesicles from each other by the vesosome outer bilayer has little effect on the vesicle fusion, and indeed may have a slight inhibitory effect on vesicle to vesicles fusion.

Adding 50 mole % charged dihexadecyldimethylammonium bromide (DHDMA<sup>B</sup>) to the DSPC-Chol interior vesicles slows the 1-month fusion rate to about 3-4% for the free vesicles and for the vesicles in vesosomes. The DHDMA<sup>B</sup> induces an electrostatic repulsion for both encapsulated and unencapsulated vesicles, which leads to the lower rate of fusion. Extruding the vesosomes to reduce their size apparently leads to a small amount of initial fusion (~2%) for both charged and uncharged vesicles as does the initial vesosome formation (~1.5%); but after this, the vesosome is quite stable. Overall, it appears that the vesosome structure is equally stable to fusion, both during construction and during storage, as simple unilamellar vesicles.

### Modifications to the Vesosome Structure

The number of bilayers and the size of the structures formed from interdigitated sheets can be modified by different cholesterol and ethanol concentrations. Fig. (8A) shows the structures formed from interdigitated sheets made from a 97.5:2.5 (mol:mol) DPPC/Chol mixtures after addition of 3M ethanol. The sheets were added to a 50

mg/ml dispersion of 50 nm DSPC/Chol (2:1) vesicles and heated to 46°C for 20 minutes. The TEM images reveal multilayer structures with multiple large internal vesicles, as well as the smaller 50 nm vesicles, all within the exterior membrane. These multi-compartmental structures are typical for this DPPC/Chol ratio. As before, the small vesicles are encapsulated at a density equal to that in the bulk solution; however, they can be trapped within multiple encapsulating bilayers in a single step. In fact, just heating the DPPC/Chol interdigitated sheets gives a multicompart structure in a single step (Fig. (8B)). Controlling the number of encapsulating membranes and the extent of compartmentalization could be important to extended drug release.

Larger structures can also be encapsulated as shown in Fig. (9). Vesicle aggregates were made by cross-linking 50 nm diameter DSPC/Chol (2:1 mol:mol) vesicles that incorporated biotin-X lipid in the bilayer with avidin [53]. The aggregates, which were many microns in size, were added to DPPC sheets (with the final lipid concentration being approximately 100 mg/ml), briefly vortexed, and heated to 46°C for 20 minutes. Fig. (9) shows that a significant fraction of the vesicle aggregates are encapsulated within the interdigitated sheets. These composite structures vary in size from 1 - 3 μm, are tightly packed with interior vesicles, and usually have a single exterior membrane (although some multilamellar shells were seen). The large aggregates are loosely crosslinked and can easily rearrange [54], allowing the spherical outer bilayer shells to form.

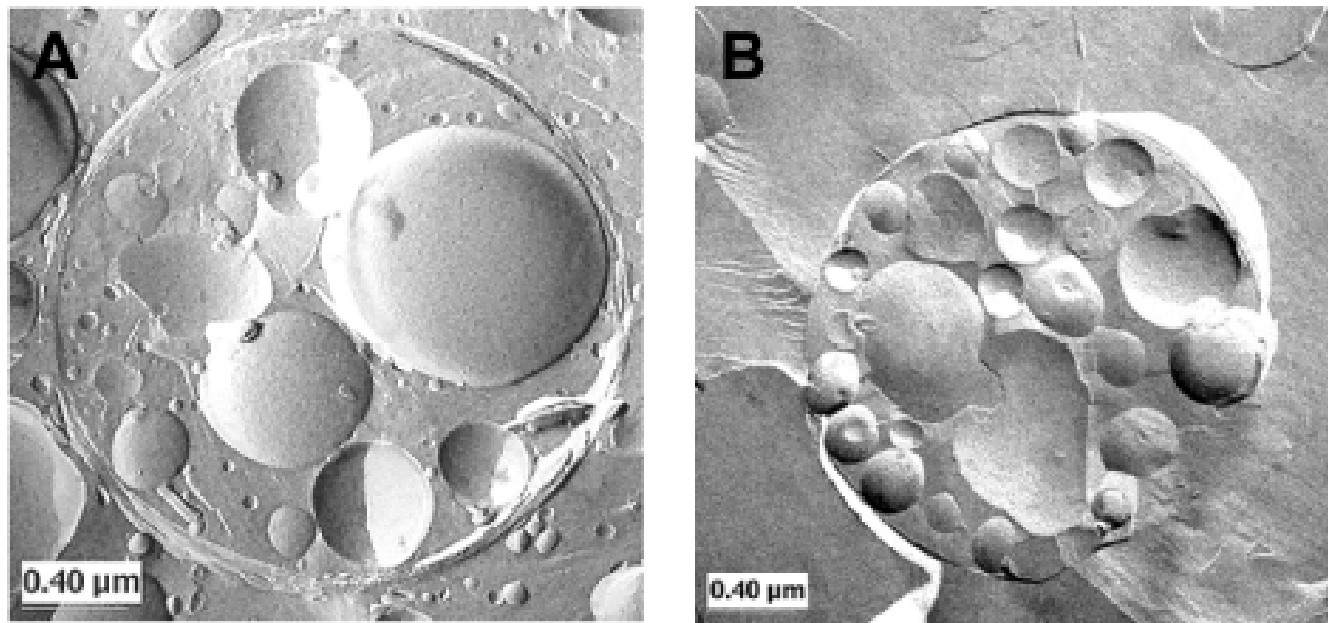


**Fig. (8).** (A) TEM image of a multicompart structure formed by adding 50 nm DSPC/Chol (2:1) vesicles to a solution of interdigitated sheets made of DPPC/Chol (97.5:2.5 molar ratio - fused with 3M EtOH) after heating to 46°C for 20 minutes, then allowing the solution to cool to room temperature. Typical structures formed from this lipid mixture had multiple small vesicle compartments inside one of more exterior bilayers. The 50 nm vesicles were added at a concentration considerably less than the solutions shown in Fig. (4A) (50 mg/ml vesicles as opposed to 200 mg/ml vesicles). However, as before, the small vesicle density is roughly equal inside and outside. The encapsulation procedure appears to be independent of the composition of the outer membranes.

(B) TEM image of a one step multicompart structure made by heating interdigitated sheets made of DPPC/Chol (97.5:2.5 molar ratio) fused with 3M EtOH to 46°C.

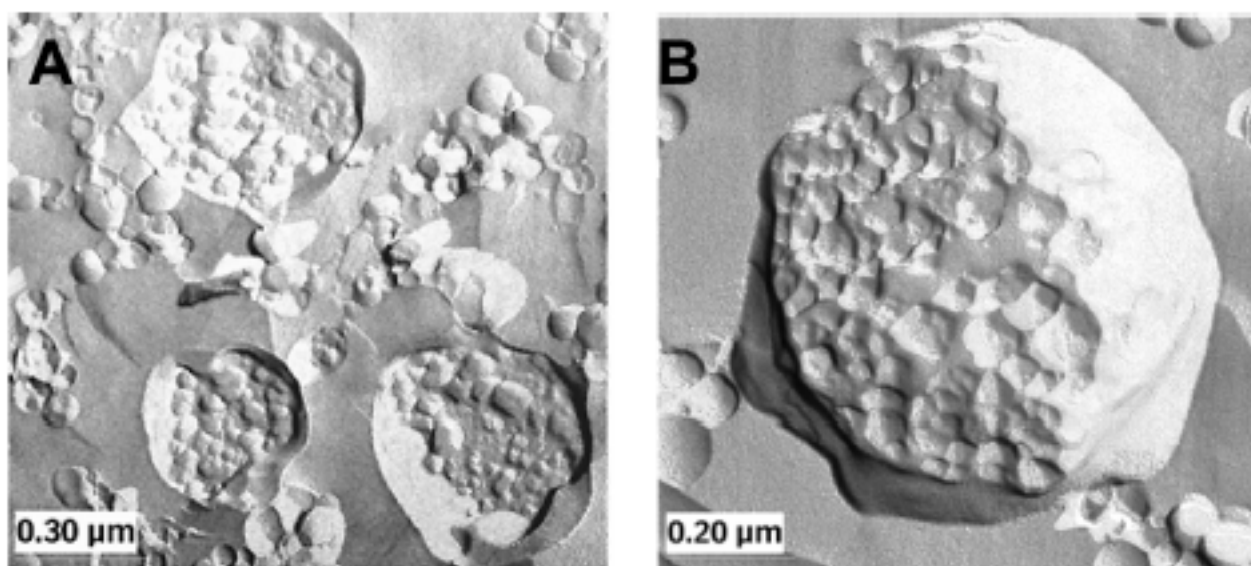


**Fig. (9).** TEM images of vesosomes formed after adding micron sized vesicle aggregates (crosslinked with biotin and avidin) to interdigitated sheets of DPPC and heating to 46C for twenty minutes. Encapsulated vesicles have retained their size (~ 50 - 70 nm) and compact packing.

#### Colloidal Particles

Stabilizing colloidal particles against flocculation in biological or other high ionic strength environments is also possible with this encapsulation scheme. Small particles of various metals, oxides, etc ( $\text{TiO}_2$ ,  $\text{Fe}_2\text{O}_3$ , Au) can be formed with quite narrow size ranges and dispersed in a low ionic strength aqueous environment [55]. However, the small particles often flocculate at biologically relevant electrolyte concentrations and must be stabilized by polymers, surfactants or other additives to be used *in vivo* [55]. It is also possible to stabilize colloidal particles against flocculation by encapsulating them in a vesosome, Fig. (10).

30 nm  $\text{TiO}_2$  particles were suspended in pure water at pH 8 and dispersed by brief sonication. The sonicated suspension is stable for days over a range of 1- 15 weight%  $\text{TiO}_2$ . However, increasing the ionic strength to 0.01 M causes the suspension to flocculate immediately. A stable suspension of 7.5 wt%  $\text{TiO}_2$  was prepared in pure water and mixed with interdigitated DPPC sheets, also prepared in pure water at pH 8. The solution was heated to 46° C as described above to encapsulate the suspended  $\text{TiO}_2$ . Immediately after encapsulation, 0.1 M salt was added to the solution causing all of the unencapsulated  $\text{TiO}_2$  to flocculate and sediment, leaving a clear supernatant. The vesosomes were initially dragged down to the bottom of the vial by the

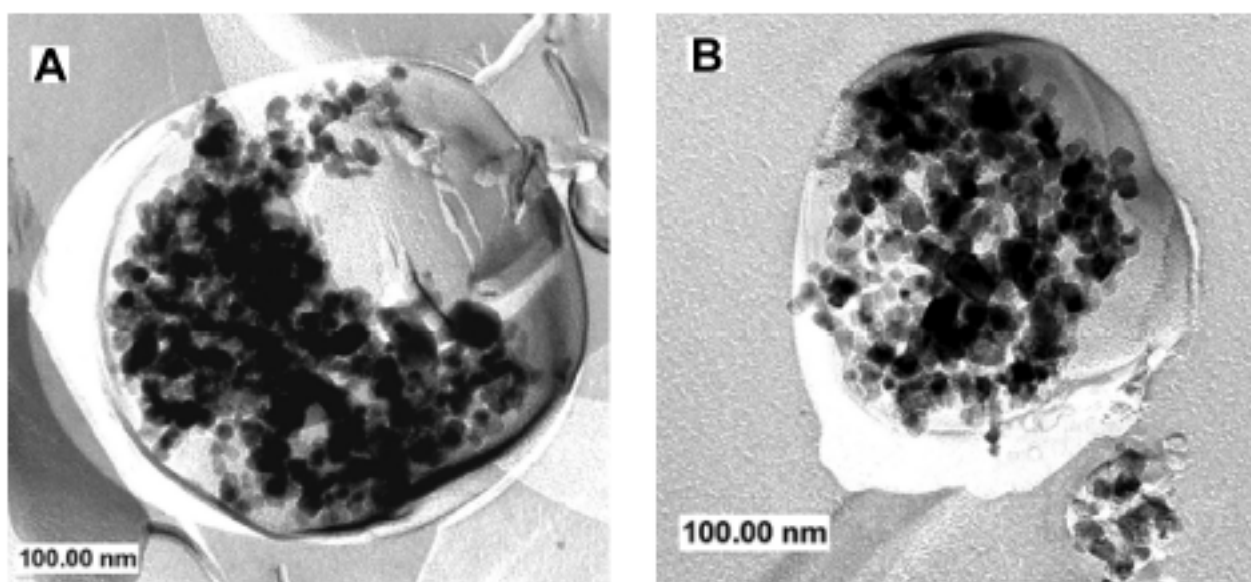


**Fig. (10).** A, B. TEM images of 7.5 wt% colloidal titanium dioxide solution in water at pH 8 encapsulated within interdigitated DPPC bilayers. The black,  $\text{TiO}_2$  particles are clearly within the bilayer outlines in the image showing that they were encapsulated. Bilayer encapsulation appears to be a novel method of stabilizing a colloidal dispersion in a biological environment.

rapid sedimentation of the TiO<sub>2</sub>. After about 24 hours, the vesosomes spontaneously separated from the flocculate and reappeared in the supernatant. Fig. (10) shows small clusters of TiO<sub>2</sub> particles encapsulated within bilayer membranes by this process. The exterior bilayer of the vesosome limits the flocculation of the TiO<sub>2</sub>, and the density of the flocs inside the vesosome are sufficiently low that the vesosomes can remain suspended in solution. Essentially any colloidal particle could be encapsulated within a bilayer membrane to enhance its stability in solution, including magnetic particles for separations, drug targeting, or contrast enhancement for MRI [19,20,56-58].

### DNA Encapsulation

DNA contained within or condensed by cationic liposomes [59-64] penetrates anionic cell membranes relatively easily in culture. The transfection efficiency of cationic lipoplexes is greater than DNA delivered by other lipids [65,66] but considerably lower than DNA delivered in a viral envelope [67,68]. Additionally, poor reproducibility of transfection [69,70] may be caused by variability of the structure and size of the liposome-DNA complexes [71]. *In vivo*, the charged complexes are toxic and have immunoadjuvant activity [72] prior to their rapid clearance from circulation by nonspecific interactions with blood proteins [73,74].

One way of mitigating the adverse effects of the cationic condensing agent is to encapsulate the condensed genetic material in negative or neutral phospholipids. For example, plasmid DNA precondensed with spermidine was enclosed in negative liposomes via a solvent emulsification process known as reverse phase evaporation and subsequently

reduced in sized by extrusion through filters [75,76]. A solvent-containing emulsion was also the route for enclosing antisense oligodeoxynucleotides condensed with a cationic lipid in neutral vesicles [77]. Semple *et al.* presented an alternative method of obtaining a neutral outer envelope [78]. They enclosed antisense oligonucleotides in positive vesicles of pH-sensitive lipids that were then extruded and made neutral by an increase of pH. Simultaneous condensation and encapsulation of plasmid DNA were accomplished by Bailey and Sullivan, who added ethanol and calcium to mixtures of plasmid and small, neutral phospholipids [79].

While these approaches do allow shielding of genetic material by negative or neutral phospholipids, the mechanisms of liposome formation can be problematic. DNA is easily damaged by sonication or extrusion, and reverse phase evaporation of emulsions involves solvents that may degrade DNA [80]. Moreover, any new lipids and processes would require extensive safety testing prior to *in vivo* use. An alternative would be to encapsulate condensed DNA within neutral bilayers of DPPC by the vesosome process. Spermidine is a naturally occurring trivalent cation at physiological pH [81,82] that condenses DNA in dilute solutions into toroids or rod-like structures [83-86] small enough to be efficiently encapsulated during the conversion from interdigitated DPPC sheets to closed, bilayer vesicles.

To prepare DNA-vesosomes, pGL3-luciferase control vector plasmid DNA (pGL3-luc CV, 5256 bp) in a low salt buffer containing 10 mM TES and 1 mM NaCl adjusted to pH 7.4. DNA was condensed prior to encapsulation by the addition of a 250 mM spermidine solution to a final concentration of 25 µg/mL DNA and 10 mM spermidine. The DNA was encapsulated by first adding 30 µL of the

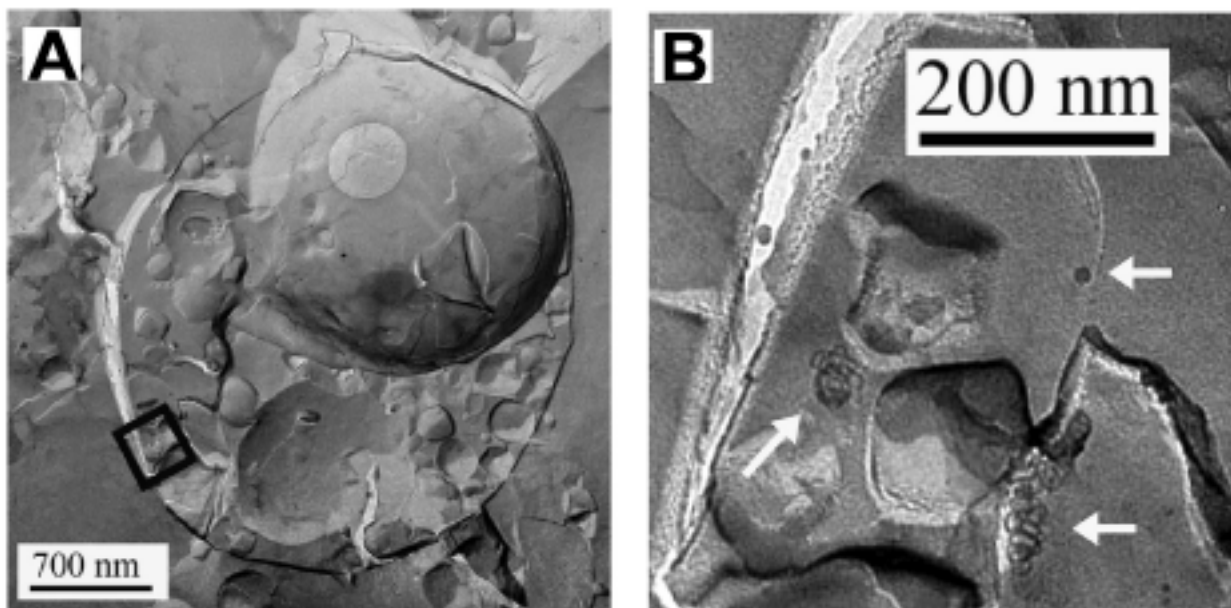


Fig. (11). Freeze-fracture TEM images of condensed DNA encapsulated within DPPC vesosomes.

(A). View of the entire vesosome structure, which has small vesicles of DPPC and condensed DNA surrounded by an outer envelope of DPPC.

(B). A higher magnification view of the region within the box of (a), in which toroids of condensed, encapsulated DNA are indicated by arrows.

suspension of condensed DNA to the DPPC interdigitated sheets, followed by brief vortexing to mix the sheets and DNA. Heating at 60° C for 20 minutes caused the DPPC sheets to form spherical bilayers and passively encapsulate the condensed DNA, (Fig. (11)). Although heating at 46° C is typically sufficient to generate vesosomes from interdigitated sheets, the higher temperature was necessary to anneal defects in the presence of 10 mM spermidine.

The encapsulation efficiency was determined by a nuclease digestion assay. DNA remaining outside the DPPC liposomes was uncondensed by dialyzing the spermidine vs. buffer. DNase I was added to one fraction, and the reaction was stopped six hours later. The concentration of DNA remaining in this aliquot as well as the total concentration of DNA present in an undigested aliquot were determined by a fluorescence assay. When the concentrations of DPPC and DNA were 25 mg/mL and 25 µg/mL, respectively, the efficiency of protection of DNA from nuclease digestion was  $65.1 \pm 19.4\%$  ( $n = 3$ ), similar to the efficiency at which vesicles were encapsulated (Table 1).

This passive method of DNA encapsulation presents several possible advantages. Once the genetic material is added, vesosome formation does not require exposure to solvents, sonication, or extrusion. DPPC is less toxic than cationic liposomal vectors containing DOPE [72] and has a much longer circulation time in a physiological environment. Also, nonionic liposomes are more efficient than cationic vesicles for transdermal gene delivery. [87] The composition of the neutral outer bilayer could easily be varied to include cholesterol, [88] antibodies for targeted delivery, or PEG-lipids that sterically stabilize the vesosomes as shown in Fig. (5) [89]. Future experiments will test the transfection efficiency of the DNA-vesosomes.

### Models of Drug Release from Liposomes and Vesosomes

These release studies highlight a less understood feature of liposome drug delivery: the mechanisms of drug release *in vivo*. Leakage of a variety of hydrophilic, charged molecules (such as ciprofloxacin, vincristine, doxorubicin, and fluorescent charged dyes such as carboxyfluorescein) from unilamellar liposomes is often extremely slow (days to weeks to months) in buffer [90], while uncharged molecules equilibrate within hours [91,92]. This, as discussed earlier, is the basis of pH loading of weakly basic drugs [3,21]. The rate of release is consistent with the slow permeation of the charged molecules through the oily core of the membrane [93]. The flux from a unilamellar liposome is generally modeled as a simple first order process limited by the permeability through the liposome bilayer:

$$V \frac{d[C_i]}{dt} = -AP([C_i] - [C_e]) \quad (2)$$

$V$  is the internal volume of the liposome ( $4\pi R^3/3$  in which  $R$  is the vesicle radius),  $A$  is the surface area of the vesicle ( $4\pi R^2$ ),  $[C_i]$  and  $[C_e]$  are the drug concentrations inside and outside the liposome, respectively.  $P$  is the solute permeability coefficient, which is generally a function of temperature, solute, and lipid membrane composition. For

the typical case of  $[C_e] \sim 0$ , the solution of Eqn. 2 is simply:

$$[C_i] = [C_{i,initial}] \exp\left(\frac{-3Pt}{R}\right) \quad (3)$$

$$Flux = AP [C_{i,initial}] \exp\left(\frac{-3Pt}{R}\right) \quad (4)$$

$[C_{i,initial}]$  is the amount of drug in the liposome at time 0, and the  $Flux$  is the total amount of drug released per unit time. The half-life,  $t_{1/2}$ , of a drug in a liposome is then  $t_{1/2} = \ln 2/3P$ . For the 100 nm radius vesicles common to drug delivery, a half life of about 1 day requires that  $P < 3 \times 10^{-11}$  cm/sec. Experimental measurements for the permeability of potassium and sodium ions through monounsaturated phospholipid bilayers are of order 10–12 cm/sec, while anions like chloride, bromide and iodide are of order 10–9 cm/sec [93].

Drug release by permeation from the vesosome can be modeled as release from one interior vesicle with the equivalent bilayer area,  $A_v$ , total internal volume,  $VV$ , and permeability,  $P_v$ , as the encapsulated vesicles, surrounded by an outer shell of area  $A_s$  and permeability,  $P_s$ :

$$V_{in} \frac{d[C_v]}{dt} = A_v P_v ([C_v] - [C_{in}]) - A_s P_s ([C_{in}] - [C_e]) \quad (5)$$

$[C_v]$  is the drug encapsulated within the inside vesicle,  $[C_{in}]$  is the drug concentration in the interstitial space,  $V_{in}$  is the interstitial volume, and  $[C_e]$  is the drug concentration outside the vesosome. For the typical case of  $[C_e] \sim 0$ :

$$\frac{d[C_{in}]}{dt} = k_1 [C_v] - (k_1 + k_2) [C_{in}] \quad (6)$$

where  $k_1 = AV P_v / V_{in}$  and  $k_2 = AS P_s / V_{in}$ . However,  $[C_v]$  is coupled to  $[C_{in}]$  by a concentration balance of the drug in the interior of the encapsulated vesicle:

$$\frac{d[C_v]}{dt} = k_3 ([C_{in}] - [C_v]) \quad (7)$$

where  $k_3 = AV P_v / VV$ . Solving the coupled equations for the case that the initial concentration in the interstitial space,  $[C_{in}(0)] = 0$  gives [48]:

$$[C_{in}] = \frac{-[C] k_1 \left( \exp\left(\frac{x - \sqrt{z}}{2}\right) t - \exp\left(\frac{x + \sqrt{z}}{2}\right) t \right)}{\sqrt{z}} \quad (8)$$

where  $[C]$  is the initial concentration of the interior vesicle,  $x = -(k_1 + k_2 + k_3)$  and  $z = x^2 - 4k_2 k_3$ . The flux from the vesosome is [48]:

$$Flux_{ves} = \frac{-[C] A_s P_s k_1}{\sqrt{z}} \left( \exp\left(\frac{x - \sqrt{z}}{2}\right) t - \exp\left(\frac{x + \sqrt{z}}{2}\right) t \right) \quad (9)$$

To illustrate Eqn. 9, Fig. (12) shows the release from a model spherical liposome having  $P = 1.5 \times 10^{-11}$  cm/s,  $C =$

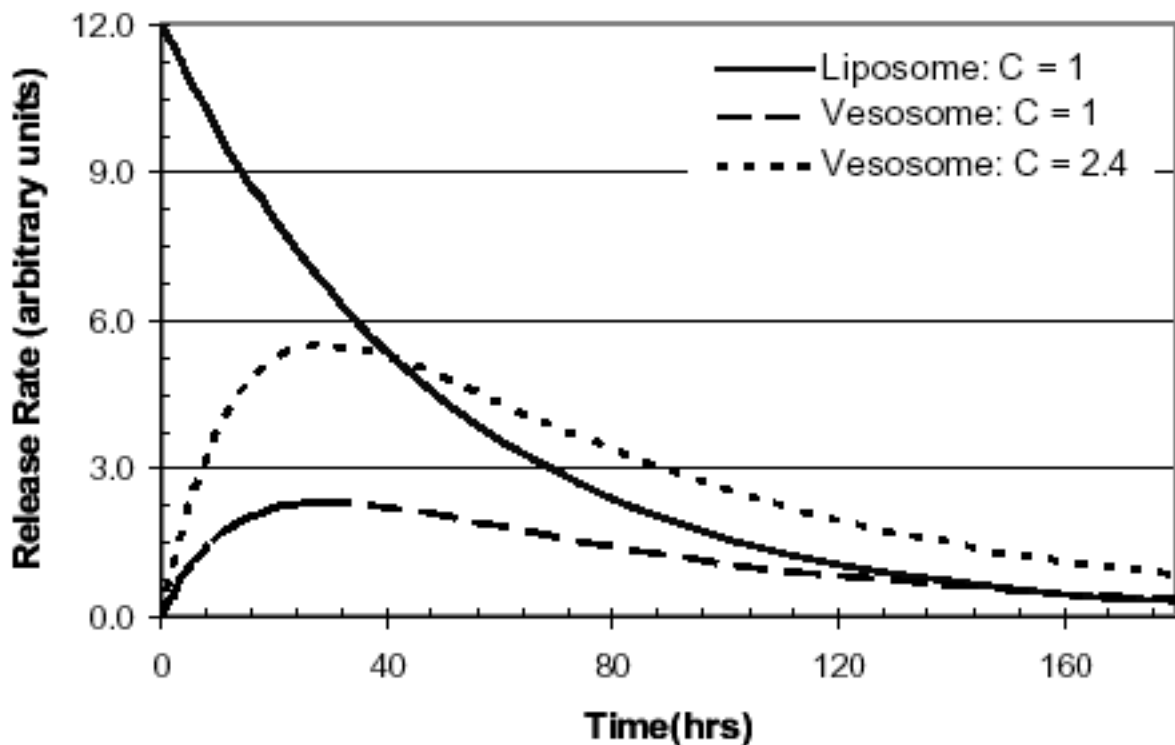


**Fig. (12).** Predicted model drug release from a spherical liposome having  $P = 1.5 \times 10^{-11}$  cm/s, an internal drug concentration of  $[C] = 1$  (arbitrary units), and a radius,  $R = 80$  nm. This is compared to a vesosome with equal permeabilities of the interior and exterior shells of  $1.5 \times 10^{-11}$  cm/s, an external shell radius,  $R_S = 80$  nm, and an internal vesicle with radius  $R_V = 60$  nm, and  $[C] = 1$  or 2.37 (arbitrary units). Only the interior vesicle in the model vesosome is loaded with drug (i.e.  $[C_{in}] = 0$ ), so the vesosome with  $[C] = 1$  has less total drug encapsulated than the model liposome. For  $[C] = 2.37$ , the vesosome contains the same total amount of drug as the liposome. Drug release from the vesosome shows a slow rise to a maximum release and a much smaller decrease with time than the simple exponential release of the liposome. The vesosome release profile could be very useful for passive or active targeting as the vesosome releases much less drug after initial injection than the liposome, allowing the vesosome to accumulate in the target tissues prior to drug release.

1 (arbitrary units), and a radius,  $R = 80$  nm. This is compared to a vesosome with  $P_S$  and  $P_V = P = 1.5 \times 10^{-11}$  cm/s, an external shell radius,  $R_S = 80$  nm, and an internal vesicle with radius  $R_V = 60$  nm, and  $[C] = 1$  or 2.37 (arbitrary units). As only the interior vesicle in the model vesosome is loaded with drug (i.e.  $[C_{in}] = 0$ ), the vesosome with  $[C] = 1$  has less total drug encapsulated than the model liposome. For  $[C] = 2.37$ , the vesosome contains the same total amount of drug as the liposome.

Fig. (12) shows that release from the vesosome has a start-up period in which little drug is released, as the interstitial space is originally empty. As the interstitial space begins to fill, drug release begins into the surroundings. The release rate reaches a maximum before decreasing to a slow, steady decline. This is quite different from release from a conventional liposome. The liposome immediately releases drug at its maximum rate, followed by an exponential decay according to Eqn. 4. This large variation in release is not optimal for best efficacy, especially if passive targeting is to be employed. After injection of the liposomes, it takes time for the liposomes to circulate through the circulatory system and passively target a tumor site. During this time, the liposome is releasing drug at its maximum rate, decreasing the availability of the drug at the tumor (and causing unwanted toxic side effects). On the other hand, the vesosome does not display this initial release spike. By the

time the vesosome has reached its maximum release rate, the vesosomes should have had sufficient time to circulate through the bloodstream and passively target the tumor. This should lead to a higher bioavailability of the drug at the tumor. At least in theory, a vesosome could be loaded with less drug than a liposome, but still deliver a larger drug dose at the tumor site. Furthermore, the vesosome displays a more constant and controllable release rate over a longer period – unlike the exponentially decaying release that all liposomes follow.

#### Small Molecule Release from Liposomes and Possible Vesosome Advantages

Although it is possible to make and load stable vesosomes quite efficiently, there must be an essential benefit for the added complexity of the structure to compete with conventional unilamellar liposomes. The simple release model outlined above shows that the drug delivery profiles can be improved by the nested structure of the vesosome. More importantly, the multiple barrier structure of the vesosome directly addresses one of the major problems with conventional liposomes, the overly fast release rates of most drugs in serum [21,94-97], especially when compared with the release of the same drugs in isotonic saline.

We have used the self-quenching of carboxyfluorescein (CF) to study the release of hydrophilic, charged molecules from liposomes and vesosomes in saline and blood serum [52]. CF is retained in 100 – 200 nm diameter unilamellar liposomes for about 1 month at room temperature and for greater than 7 days at 37° C, similar to charged drugs like ciprofloxacin and vincristine [35]. To measure the release of CF from unilamellar liposomes and vesosomes in the presence of serum, we modified the method of Johnson and Bangham [98,99]. As a control, we compared the release from unilamellar liposomes made from DSPC. The vesosomes made from similar 50 nm diameter DSPC vesicles encapsulated in DPPC sheets. Both the control vesicles and the vesicles to be encapsulated were made in a 20 mmol carboxyfluorescein (CF) solution. Excess carboxyfluorescein was removed by rapidly dialyzing through a 300,000 molecular weight cut-off (MWCO) cellulose ester dialysis bag twice against a 100:1 bath volume at room temperature until negligible CF was detected in the external solution by observing the fluorescence emission at 517 nm after excitation at 492 nm.

The dialyzed 50 nm DSPC vesicles containing the quenched CF were mixed with interdigitated DPPC sheets, followed by heating for 30 minutes at 46° C to form vesosomes. Vesosomes were separated from non-

encapsulated vesicles via centrifugation. CF release was initiated by mixing an equal volume of the control vesicles or vesosomes with bovine serum (Sigma, St. Louis, MO). This mixture was placed in a cellulose ester dialysis bag (5,000 MWCO) and allowed to dialyze into a 100:1 by volume isotonic 1:5 bovine serum:HEPES buffer bath held at 37° C. The vesicles, vesosomes and serum proteins should remain in the 5,000 molecular weight cut off bag, while CF passes freely across the dialysis membrane. Samples were drawn off periodically from the exterior bag and measured for fluorescent intensity. At the concentrations used, the CF showed a linear relationship of fluorescence intensity with concentration. At the end of the experiment (~ 50 hrs), sufficient Triton-X detergent was added to the dialysis bag to completely lyse the liposomes or vesosomes and release any remaining CF. To ensure total release, we allowed the dialysis bag to equilibrate within the buffer bath until a constant fluorescence intensity was obtained. This final CF concentration is taken to be the total entrapped CF in the control liposomes or vesosomes. The relative amount of CF release is calculated as the ratio of the CF concentration measured at various times to the end-point concentration. While there is a lag-time for CF to equilibrate across the dialysis membrane, both vesicle and vesosome samples are exposed to a similar lag-time.

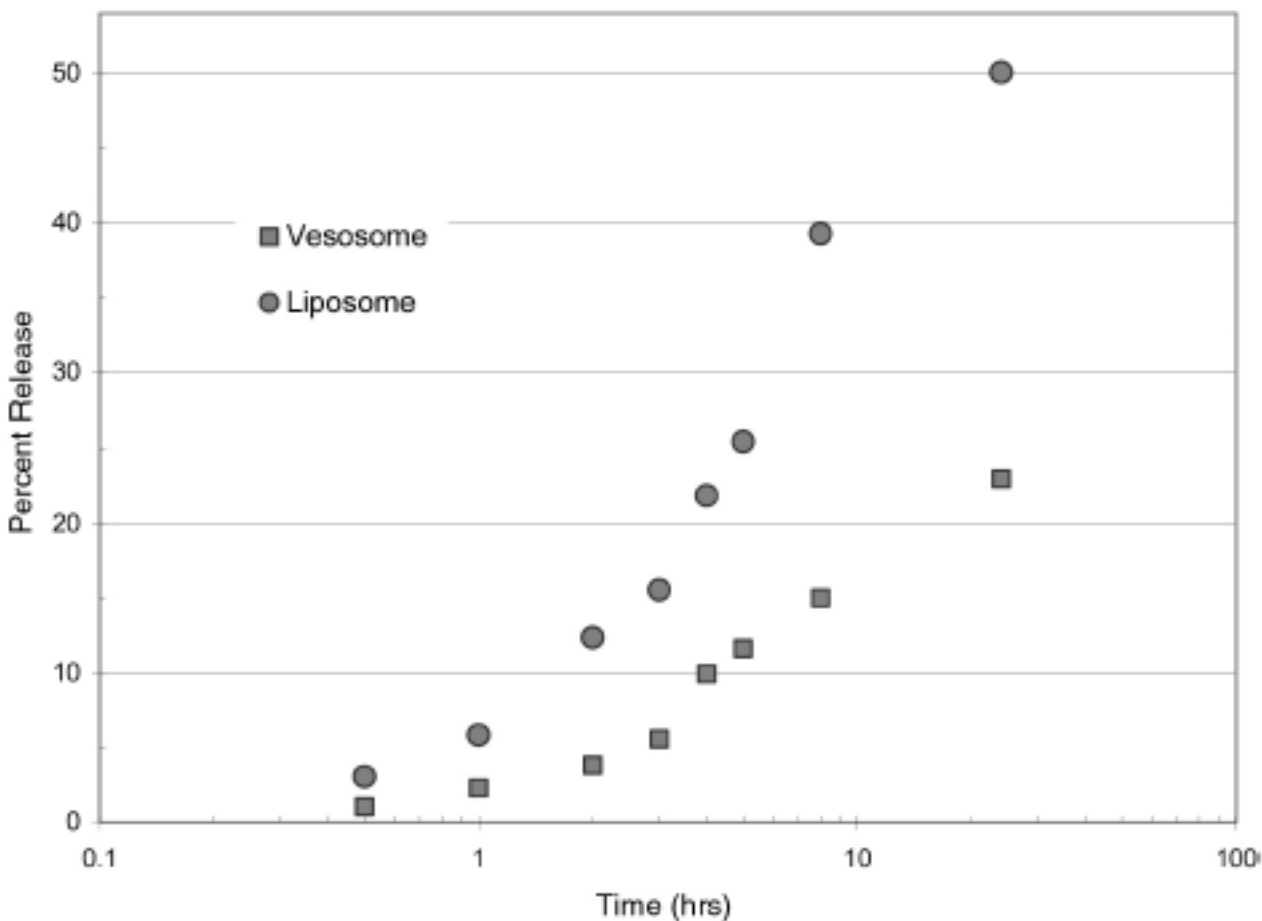


**Fig. (13).** CF release rates from conventional unilamellar liposomes of distearoylphosphatidylcholine (DSPC) and DSPC encapsulated vesosomes in 50% bovine serum at 37° C. In comparison to the multicompartiment vesosomes, unilamellar vesicles have much faster initial CF release as predicted. 20% drug release occurs in about 3 hours from the liposomes and about 24 hours from the vesosomes.

Fig. (13) shows CF release from the DSPC unilamellar liposomes compared to DSPC encapsulated vesosomes. The unilamellar liposomes release more than 20% of the water soluble CF in about 3 hours in 50% bovine serum at 37° C. However, for similar DSPC encapsulated vesosomes, 20% release takes ~ 24 hours. This is a significant difference in release rates, and is greater than that expected for simple permeation through multiple membranes. This is especially true because the permeation across the DPPC outer membrane should be considerably faster than the permeation through a DSPC membrane. Furthermore, the initial release from the vesosome is quite slow, in agreement with the predictions of the permeation model discussed above and in Fig. (12). This lag time with almost no CF release may be very beneficial to a passively targeted vesosome – little drug would be released systemically for many trips through the circulation leaving a higher fraction of the drug to accumulate in tumors or inflamed sites.

### Permeation Models: Membrane Solubility vs Pore Formation

The general observation that liposomes and vesosomes release small molecules much faster in serum than in saline suggests that the permeability of the bilayer is decreased due to interactions with serum components. Two models of bilayer permeability are common in the literature, the “solubility” model and the “pore formation” model. The “solubility” model suggests that molecules to be transported across the bilayer must first “dissolve” into the bilayer, then diffuse across the bilayer and be released into the external medium. In this model, the magnitude of  $P$  for transport through a bilayer membrane is [93,100-103]:

$$P = \frac{DH}{l} \quad (10)$$

in which  $D$  is the diffusivity of the molecule in the bilayer,  $l$  is the thickness of the bilayer, and  $H$  is the partition coefficient between the water and oily interior of the bilayer. For charged and uncharged molecules of similar size, the diffusion through the bilayer interior should be roughly similar, and  $D$  should not vary much between anions, cations or neutral species.  $D$  increases with increased bilayer fluidity and is influenced by defects in the chain packing and degree of order in the bilayer [17,104,105]. Permeation is generally higher in fluid membranes than in gel state bilayers, but often is at a maximum near the gel-liquid crystal transition temperatures due to lipid packing defects or coexistence of multiple phases [17,104]. For a number of charged and uncharged species in aqueous solutions, the permeability coefficient decreases linearly with increasing lipid chain length, and hence, bilayer thickness, as predicted by Eqn. 11 [93].

In the solubility model, the origin of the difference in permeability between charged and uncharged molecules is the large difference in the partition coefficient between the water and bilayer phases,  $H$ . The bilayer creates a sheath of low dielectric permittivity (dielectric constant,  $\epsilon_b \sim 3$ ) between two aqueous regions of dielectric constant,  $\epsilon_w \sim 80$ . The solvation energy difference between an ion in water

compared to the bilayer interior is given by the Born model [93,100-102]:

$$\Delta E_{solv} = \frac{q^2}{8\pi\epsilon_0 r_{ion}} \left[ \left( \frac{1}{\epsilon_b} \right) - \left( \frac{1}{\epsilon_w} \right) \right] - \frac{q^2}{4\pi\epsilon_0 \epsilon_b d} \ln \left( \frac{2\epsilon_w}{\epsilon_w + \epsilon_b} \right) \quad (11)$$

in which  $q$  is the elementary charge,  $1.6 \times 10^{-19}$  Coulombs (C), and  $\epsilon_0$  is the permittivity of vacuum,  $8.854 \times 10^{-12}$  C<sup>2</sup>/(Joule-meter),  $r_{ion}$  is the radius of the ion, about 0.4 nm, and  $d$  is the bilayer thickness, about 5 nm. The first term in Eqn. 12 is the energy change on taking a bare ion from a solution of dielectric constant  $\epsilon_w$  into one of  $\epsilon_b$ ; the second term is the reduction in this energy due to the finite thickness of the bilayer and the resultant image charges. Eqn. 12 gives a solvation energy per molecule of about  $8.2 \times 10^{-20}$  Joules. The partition coefficient, which is the ratio of the ion concentration in the bilayer interior,  $C_b$ , to the ion concentration in the bulk water phase,  $C_w$ , can be determined by using a Boltzmann factor describing the energy difference of the ion in the water vs the bilayer interior:

$$H = \frac{C_b}{C_w} = \exp \left( \frac{-\Delta E_{solv}}{k_B T} \right) \quad (12)$$

$k_B$  is Boltzmann's constant,  $1.381 \times 10^{-23}$  Joules/K (Avogadro's number,  $N_A$ , times  $k_B$  equals the gas constant,  $R$ :  $k_B N_A = R$ ) and  $T$  is the absolute temperature in K. From this, the partition coefficient for singly charged ions of radius 0.4 nm in a bilayer of dielectric constant 3 is  $H = 4 \times 10^{-8}$ . For an ion radius of 0.2 nm, this drops to  $H \sim 10^{-18}$ . Hence, the huge variation in partition coefficients between ions and neutral species is responsible for the significantly lower permeability of ions through bilayer membranes in the solubility model. As can be seen from the calculations,  $H$  is very sensitive to rather small differences in ion radius, the actual dielectric constant of the bilayer interior, etc. [93,100,101]. More subtle electrostatic effects such as the dipole charge of the lipid bilayer can be used to explain the difference in permeability between cations and anions [93].

### Serum vs Saline Release

From the “solubility” model outlined above, it is difficult to reconcile the enormous change in the release of carboxyfluorescein, vincristine, etc. from liposome carriers when serum is used instead of buffer as the external medium, Fig. (13) [23,35,36]. No major differences are expected in any of the relevant parameters in Eqns. 10-12 on changing isotonic saline for serum. Hence, the mechanism of permeation must be fundamentally different. The “pore” model assumes that permeation occurs primarily through transient or stable defects in the bilayer produced by thermal [105] or chemical fluctuations or by specific species that assist in the formation or stabilization of pores [93,99]. By passing through water-filled pores in the bilayer, the permeating molecule can avoid the high cost of partitioning into the low dielectric constant interior of the bilayer (Eqns. 11-12) [93,100]. The increase in permeability due to pores

and defects will be greatest for the charged molecules that have the lowest solubility in the hydrophobic interior of the bilayer. Uncharged molecules may permeate via the solubility mechanism, while charged molecules may switch from solubility to pore transport depending on the density of pores relative to the bilayer dielectric properties.

A simplified model of permeation through transient pores was proposed by Hamilton and Kaler [99]. The basic concept is that the molecules trapped inside the liposome are constantly bouncing off the bilayer wall and the flux through the wall is the product of the number of ions hitting the bilayer multiplied by the fraction of the bilayer area with pores sufficiently large for the ions to get through the bilayer. The permeability coefficient can be expressed as a function of bilayer thickness and ionic radius as:

$$P = \frac{D_{\text{eff}} \gamma n_{\text{a}} RT}{R_{\text{v}} A k_1} \left[ a_i + \frac{RT}{k_1} \right] \exp \left[ \frac{-(k_1 a_i + k_2 d)}{RT} \right] \quad (13)$$

in which  $D_{\text{eff}}$  is the diffusion of the ion in water (or other medium),  $\gamma$  is the concentration enhancement due to electric double layers at the membrane surface (the concentration of charged ions of a given sign can be significantly reduced at a similarly charged surface [55]),  $A$  is the surface area of the bilayer per volume of solution,  $R_{\text{v}}$  is the radius of the vesicle,  $R$  is the gas constant,  $n_{\text{a}}$  is the maximum number of discrete pores that could exist in the bilayer.  $n_{\text{a}}$  should be proportional to the area of the bilayer, and likely is a maximum near phase transitions [17,104].  $a_i$  is the minimum cross-sectional area required for the pore to allow a given ion to pass through, and  $d$  is the thickness of the hydrophobic part of the bilayer. The constant  $k_1$  is the energy/area associated with the formation of a pore of area  $a_i$  and  $k_2$  is the energy/length associated with the formation of a pore of depth  $d$ . This model suggests that any mechanism by which  $k_1$  and  $k_2$  might be lowered should dramatically increase the permeability.

The energy of pore formation can be estimated from the Helfrich theory of bilayer deformations [106]. The pore is modeled as a toroidal shaped perforation of the bilayer:

$$g_{\text{pore}} = (k_1 a_i + k_2 d) = \left[ \frac{\kappa}{2} (c_1 + c_2 - c_0)^2 + \frac{\bar{\kappa}}{2} c_1 c_2 \right] a_{\text{wall}} \quad (14)$$

$\kappa$  and  $\bar{\kappa}$  are the bend and saddle-splay elastic constants of the bilayer. For many bilayer forming phospholipids,  $\kappa$  and  $\bar{\kappa}$  are of order 10-12 ergs and increase with bilayer thickness, and hence, the chain length of the phospholipids [107-110]. Mixtures of lipids generally have lower values of  $\kappa$  and  $\bar{\kappa}$  than do single component bilayers as the local bilayer composition can adjust to the local curvature [109,110].  $c_1$  is the curvature of the pore wall normal to the bilayer, (approximately  $1/2d$ , or half the bilayer thickness),  $c_2$  is the curvature of the pore parallel to the bilayer ( $-1/r_{\text{pore}} \sim -(1/2d + a_i^{-1/2})$ ) and  $c_0$  is the preferred curvature of the bilayer. For typical bilayer forming, double-tailed phospholipids,  $c_0 \sim 0$ , and the bilayer prefers to be flat [55,106,109,110]. However, for micelle forming surfactants like lysolipids,  $c_0 \sim 1/2d$ , as the micelle diameter is typically two molecule lengths [55]. Non-ideal lipid mixing

within the bilayer can also lead to nonzero values of the preferred curvature [109-111], which may act to lower the formation energy of pores.

From the dramatic increase in permeability in saline relative to serum [23,35,36], it appears most likely that elements present in serum act to decrease the energy of pore formation in liposomes. There are a number of active species in serum such as lipases, enzymatic lipolytic agents, complement, and other factors that may interact specifically with various components of the bilayer. Among the common hydrolysis products of phospholipids are lysolipids and fatty acids, both of which are capable of forming micellar structures in solution [55,112]. Lysolipids are known to increase the permeation from liposomes [17,18,113], which is likely due to their ability to decrease the energy of pore formation. Adding lysolipids to the phospholipid bilayer could induce a preferred curvature similar to that of the lysolipid,  $c_0 \sim 1/2d$  rather than that of the bilayer,  $c_0 \sim 0$ . This would drastically decrease the curvature energy associated with pore formation (first term in Eqn. 8) and increase the probability for pores of sufficient size for ion permeation to occur. Addition of lysolipids or fatty acids would not alter the ion solubility in the bilayer significantly as the dielectric properties of the hydrophobic portion of the bilayer would be relatively unchanged (See Eqn. 5). As hydrolysis of the bilayer proceeds during exposure to serum, the probability of pores of sufficient size steadily increases as the fraction of lysolipids and other degradation products increases. Hence, the permeability of a liposome in serum steadily decreases with exposure to the point where the bilayer provides essentially no barrier at all to ion transport.

The pore mechanism suggests the origin of the benefit of the multiple bilayers in the vesosome. The catalytic turnover by many lipolytic enzymes occurs at the interface between the liposome (or vesosome) and the external solution (for review, see [114]). For example, during the course of hydrolysis of phospholipid vesicles by phospholipase A2, only the phospholipid molecules in the outer monolayer are hydrolyzed and the bilayer structure is retained [114]. A significant fraction of the lipid degradation products are retained within the liposome bilayer as the products are likely to be either amphiphilic (lysolipids) or hydrophobic (fatty acids). The degradation products lead to a reduction in the energy of formation of pores and the increase in the bilayer permeability to ions, but only in the particular liposome that interacted with the enzyme [114]. Other liposomes in solution not in contact with the enzyme would not undergo a similar increase in permeability.

Most lipolytic enzymes are at least 10 Kdalton in molecular weight and generally bind tightly to the bilayer surface with which they interact [114]. For such an enzyme to interact with the interior vesicles in the vesosome, the lipolytic enzyme would first have to pass through the exterior membrane of the vesosome. This would require a large pore relative to the smaller molecular weight ions or drugs that we are interested in containing. The probability of such pores decreases exponentially with pore size according to Eqns. 13 and 14, and would likely happen much more slowly than the formation of sufficient pores to equilibrate small molecular weight molecules like CF contained in

unilamellar vesicles. In addition, the enzyme would have to unbind from the bilayer surface to be transported through the pore. There are a number of interior vesicles within a vesosome, so sufficient enzyme must permeate through the exterior membrane to begin to attach and react with each interior vesicle for these vesicles to release their contents, or the interior vesicles must be degraded sequentially. Either of these mechanisms would significantly extend the release of CF from the vesosome relative to unilamellar liposomes. The vesosome provides a very interesting new substrate with which to study lipolytic enzyme catalysis of bilayers. It could be that decreased rates of small molecule release provides an important advantage for eukaryotes over prokaryotes.

## CONCLUSIONS

The above procedures provide a simple, inexpensive way to efficiently encapsulate aggregates, colloids or vesicles inside one or more continuous bilayers. The encapsulation process can entrap a variety of vesicle compositions and sizes, and it possible to encapsulate colloidal particles and sensitive biological structures such as condensed DNA stably and efficiently. The vesosome retains all of the essential features of conventional unilamellar liposomes including ease of manufacture, the possibility of extended circulation times and passive targeting to tumors or inflammation sites due to small (<250 nm) size and steric stabilization with PEG-lipids, and the ability to efficiently load weakly basic drugs with pH gradients. The vesosome also provides several important advantages over unilamellar liposomes. The interior bilayers can be of different composition from each other and from the exterior membrane. The interior vesicles bilayers can incorporate charged lipids or be decorated with other lipids that might lead to rapid aggregation if directly exposed to serum. The vesosome may contain different drugs to be delivered simultaneously in well-defined ratios. The vesosome can provide a significantly different release profile that can minimize spikes in drug release in comparison to unilamellar liposomes. Perhaps most important, the nested structure provides a significant barrier to degradation by lipolytic enzymes and other components of serum that might lead to premature release *in vivo*. Future work will determine if these benefits can be translated into clinical success for delivery of drugs that may benefit from extended release profiles in the circulation.

## ACKNOWLEDGEMENTS

Financial support for this project was provided by the National Institutes of Health grant EB-000380, the NSF Nanotechnology Integrative Research Team Grant 0103516 and the MSERC program of the NSF under grant DMR-9632716. The authors thank J. Israelachvili for his suggestions on the original design of the vesosome and ongoing collaborations.

## ABBREVIATIONS

CF = Carboxyfluorescein

Chol	=	Cholesterol
cipro	=	Ciprofloxacin
H	=	Partition coefficient between aqueous phase and bilayer
D	=	Diffusion constant
DOPS	=	Diioleoylphosphatidylserine
DPPE	=	Dipalmitoylphosphatidylcholine
DPPC-NBD	=	(1-Palmitoyl-2-[6-[(7-nitro-2-1,3-benzoxadiazol]-4-yl)amino]caproyl]-sn-Glycero-3-Phosphocholine
DSPC	=	Distearoylphosphatidylcholine
$\epsilon_b$	=	Dielectric constant of bilayer interior
$\epsilon_w$	=	Dielectric constant of water
$\kappa$	=	The bending elastic constant for a bilayer
$\bar{\kappa}$	=	The saddle-splay elastic constant for a bilayer
lyso-PC	=	Lysophosphatidylcholine
MWCO	=	Molecular weight cut-off
P	=	Bilayer permeability
PEG	=	Polyethylene glycol polymer (PEG) polymer covalently bound to a lipid
PEG-DPPE	=	PEG conjugated to dipalmitoylphosphatidylethanolamine
PEG-lipid	=	Polyethylene glycol polymer covalently bound to a lipid
TEM	=	Transmission electron microscopy

## REFERENCES

- [1] Bangham, A.D.; Standish, M.M.; Watkins, J.C. *J. Mol. Biol.*, **1965**, *13*, 238.
- [2] Lasic, D.D. *Liposomes: From Physics to Applications*, Elsevier: Amsterdam, **1993**.
- [3] Barenholz, Y. *Curr. Opin. Colloid Interf. Sci.*, **2001**, *6*, 66.
- [4] Allen, T.M. *Curr. Opin. Colloid Interf. Sci.*, **1996**, *1*, 645.
- [5] Lasic, D.D.; Barenholz, Y., Eds., *Handbook of Nonmedical Applications of Liposomes*, CRC Press, Inc.: Boca Raton, Florida, **1996**; Vol. 1-4.
- [6] Gabizon, A.; Papahadjopoulos, D. *Proc. Natl. Acad. Sci. U.S.A.*, **1988**, *85*, 6949.
- [7] Lasic, D.D.; Papahadjopoulos, D. *Curr. Opin. Solid St. Mater. Sci.*, **1996**, *1*, 392.
- [8] Allen, T.M.; Hansen, C.B.; Lopes de Menezes, D.E. *Adv. Drug Delivery Rev.*, **1995**, *16*, 267.
- [9] Connolly, D.T.; Heuvelman, D.M.; Nelson, R.; Olander, J.V.; Eppely, B.L.; Delfino, J.J.; Siegel, N.R.; Leimgruber, R.M.; Feder, J. *J. Clin. Invest.*, **1989**, *84*, 1470.
- [10] Symon, Z.; Peyser, A.; Tzemach, D.; Barenholz, Y.; Lasic, D.D. *Cancer*, **1999**, *86*, 72.
- [11] Gabizon, A. *Clin. Cancer Res.*, **2001**, *7*, 223.
- [12] Duncan, R. *Anticancer Drugs*, **1992**, *3*, 175.
- [13] Maeda, H. *Adv. Drug Delivery Rev.*, **1991**, *6*, 181.
- [14] Schiffellers, R.M.; Storm, G.; ten Kate, M.T.; Stearne-Cullen, L.E.T.; Hollander, J.G.; Verbrugh, H.A.; Bakker-Woudenberg, I. *J. Liposome Res.*, **2002**, *12*, 122.
- [15] Sapra, P.; Allen, T.M. *Cancer Res.*, **2002**, *62*, 7190.
- [16] Goren, D.; Horowitz, A.T.; Tzemach, D.; Tarshish, M.; Zalipsky, S.; Gabizon, A. *Clin. Cancer Res.*, **2000**, *6*, 1949.

- [17] Needham, D.; Dewhirst, M.W. *Adv. Drug Delivery Rev.*, **2001**, 53, 285.
- [18] Jorgensen, K.; Davidsen, J.; Mouritsen, O.G. *FEBS Lett.*, **2002**, 531, 23.
- [19] Lubbe, A.S.; Bergemann, C.; Brock, J.; McClure, D.G. *J. Magn. Magn. Mater.*, **1999**, 194, 149.
- [20] Lubbe, A.S.; Alexiou, C.; Bergemann, C. *J. Surg. Res.*, **2001**, 95, 200.
- [21] Cullis, P.R.; Hope, M.J.; Bally, M.B.; Madden, T.D.; Mayer, L.D.; Fenske, D.B. *Biochim. Biophys. Acta*, **1997**, 1331, 187.
- [22] Haran, G.; Cohen, R.; Bar, L.K.; Barenholz, Y. *Biochim. Biophys. Acta*, **1993**, 1151, 201.
- [23] Maurer, N.; Wong, K.F.; Hope, M.J.; Cullis, P.R. *Biochim. Biophys. Acta*, **1998**, 1374, 9.
- [24] Diat, O.; Roux, D. *J. Phys. II*, **1993**, 3, 9.
- [25] Kim, T.; Murdande, S.; Gruber, A.; Kim, S. *Anesthesiology*, **1996**, 85, 331.
- [26] Spector, M.S.; Zasadzinski, J.A.; Sankaram, M.B. *Langmuir*, **1996**, 12, 4704.
- [27] Kisak, E.; Coldren, B.; Zasadzinski, J.A. *Langmuir*, **2002**, 18, 284.
- [28] Evans, C.A.; Zasadzinski, J.A. *Langmuir*, **2003**, 19, 3109.
- [29] Evans, C.A.; Zasadzinski, J.A. *J. Liposome Res.*, **2003**, submitted.
- [30] Rädler, J.O.; Koltover, I.; Salditt, T.; Safinya, C.R. *Science*, **1997**, 275, 810.
- [31] Stuart, D.D.; Allen, T.M. *Biochim. Biophys. Acta*, **2000**, 1463, 219.
- [32] Senior, J.H.; Trimble, K.R.; Maskiewicz, R. *Biochim. Biophys. Acta*, **1991**, 1070, 173.
- [33] Allen, T.M.; Austin, G.A.; Chonn, A.; Lin, L.; Lee, K. *Biochim. Biophys. Acta*, **1991**, 1061, 56.
- [34] Fukusawa, M.; Adachi, H.; Hirota, K.; Tsujimoto, M.; Arai, H.; Inoue, K. *Exp. Cell Res.*, **1996**, 222, 246.
- [35] Maurer-Spurej, E.; Wong, K.F.; Maurer, N.; Fenske, D.B.; Cullis, P.R. *Biochim. Biophys. Acta*, **1999**, 1416, 1.
- [36] Webb, M.S.; Boman, N.L.; Wiseman, D.J.; Saxon, D.; Sutton, K.; Wong, K.F.; Logan, P.; Hope, M.J. *Antimicrob. Agents Chemoth.*, **1998**, 42, 45.
- [37] Bakker-Woudenberg, I.; ten Kate, M.T.; Guo, L.; Working, P.; Mouton, J.W. *Antimicrob. Agents Chemoth.*, **2001**, 45, 1487.
- [38] Embree, L.; Gelmon, K.; Tolcher, A.; Hudon, N.; Heggie, J.; Dedhar, C.; Logan, P.; Bally, M.B.; Mayer, L.D. *Cancer Chemoth. Pharm.*, **1998**, 41, 347.
- [39] Krishna, R.; Webb, M.S.; St. Onge, G.; Mayer, L.D. *J. Pharmacol. Exp. Ther.*, **2001**, 298, 1206.
- [40] Szoka, F.; Papahadjopoulos, D. *Ann. Rev. Biophys. Bioeng.*, **1980**, 9, 467.
- [41] McDaniel, R.V.; McIntosh, T.J.; Simon, S.A. *Biochim. Biophys. Acta*, **1983**, 731, 97.
- [42] Simon, S.A.; McIntosh, T.J. *Biochim. Biophys. Acta*, **1984**, 773, 169.
- [43] Ahl, P.L.; Chen, L.; Perkins, W.R.; Minchey, S.R.; Boni, L.T.; Taraschi, T.F.; Janoff, A.S. *Biochim. Biophys. Acta*, **1994**, 1195, 237.
- [44] Marsh, D. *CRC Handbook of Lipid Bilayers*, CRC Press: Boca Raton, **1990**.
- [45] Zasadzinski, J.A.; Viswanathan, R.; Madsen, L.; Garnæs, J.; Schwartz, D.K. *Science*, **1994**, 263, 1726.
- [46] Nambi, P.; Rowe, E.; McIntosh, T. *Biochemistry*, **1988**, 27, 9175.
- [47] Fromherz, P.; Ruppel, D. *FEBS Journal*, **1985**, 179, 155.
- [48] Kisak, E.T. Ph. D. Dissertation, University of California, Santa Barbara, 2001.
- [49] Papahadjopoulos, D.; Vail, W.J.; Newton, C.; Nir, S.; Jacobson, K.; Poste, G.; Lazo, R. *Biochim. Biophys. Acta*, **1977**, 465, 579.
- [50] DPPC, DPPG, DOPS, DSPC, cholesterol and 1,2 diacyl-SN-glycero-3-phosphoethanolamine - N-[Methoxy(polyethylene glycol)-2000] (PEG-2000) were purchased from Avanti Polar Lipids (Alabaster, Alabama) and used as received. Avidin and biotin-X-DPPE were purchased from Molecular Probes (Eugene, Oregon). Stearylamine and all solvents used (analytical grade or better) were purchased from Aldrich Chemical Co. (St. Louis Mo.). Lipid mixtures were made by dissolving the appropriate quantities of the lipids in chloroform.
- [51] Chiruvolu, S.; Warriner, H.E.; Naranjo, E.; Idziak, S.; Rädler, J.O.; Plano, R.J.; Zasadzinski, J.A. Safinya, C.R. *Science*, **1994**, 266, 1222.
- [52] Spence, M.T.Z., Ed., *Handbook of Fluorescent Probes and Research Chemicals*, Molecular Probes, Inc.: Eugene, Or., **1996**.
- [53] Chiruvolu, S.; Walker, S.; Leckband, D.; Israelachvili, J.; Zasadzinski, J. *Science*, **1994**, 264, 1753.
- [54] Kisak, E.; Kennedy, M.T.; Trommeshauser, D.; Zasadzinski, J.A. *Langmuir*, **2000**, 16, 2825.
- [55] Israelachvili, J.N. *Intermolecular and Surface Forces*, Academic Press: London, **1992**.
- [56] Kim, D.K.; Zhang, Y.; Voit, W.; Rao, K.V.; Kehr, J.; Bjelke, B.; Muhammed, M. *Scripta Mater.*, **2001**, 44, 1713.
- [57] Portet, D.; Denizot, B.; Rump, E.; Lejeune, J.J.; Jallet, P. *J. Colloid Interf. Sci.*, **2001**, 238, 37.
- [58] Viroonchatapan, E.; Sato, H.; Ueno, M.; Adachi, I.; Tazawa, K.; Horikoshi, I. *Life Sci.*, **1996**, 58, 2251.
- [59] Rädler, J.O.; Koltover, I.; Salditt, T.; Safinya, C.R. *Science*, **1997**, 275, 810.
- [60] Koltover, I.; Salditt, T.; Rädler, J.O.; Safinya, C.R. *Science*, **1998**, 281, 78.
- [61] Koltover, I.; Salditt, T.; Safinya, C.R. *Biophys. J.*, **1999**, 77, 915.
- [62] Koltover, I.; Wagner, K.; Safinya, C.R. *Proc. Natl. Acad. Sci. U.S.A.*, **2000**, 97, 14046.
- [63] Templeton, N.S.; Lasic, D.D.; Frederik, P.M.; Strey, H.H.; Roberts, D.D.; Pavlakis, G.N. *Nat. Biotechnol.*, **1997**, 15, 647.
- [64] Tam, P.; Monck, M.; Lee, D.; Ludkovski, O.; Leng, E.C.; Clow, K.; Stark, H.; Scherrer, P.; Graham, R.W.; Cullis, P.R. *Gene Ther.*, **2000**, 7, 1867.
- [65] Felgner, P.L.; Gadek, T.R.; Holm, M.; Roman, R.; Chan, H.W.; Wenz, M.; Northrop, J.P.; Ringold, G.M.; Danielson, M. *Proc. Natl. Acad. Sci. U.S.A.*, **1987**, 84, 7413.
- [66] Legendre, J.Y.; Szoka, F.C. *Pharm. Res.*, **1992**, 9, 1235.
- [67] Friedmann, T. *Sci. Am.*, **1997**, 276, 96.
- [68] Felgner, P.L. *Sci. Am.*, **1997**, 276, 102.
- [69] Lew, D.; Parker, S.E.; Latimer, T.; Abai, A.M.; Kuwahara-Rundell, A.; Doh, S.G.; Yang, Z.; Laface, D.; Gromkowski, S.H.; Nabel, G.J.; Manthorpe, M.; Norman, J. *Hum. Gene Ther.*, **1995**, 6, 553.
- [70] Thierry, A.R.; Lunardi-Iskandar, Y.; Bryant, J.L.; Rabinovich, P.; Gallo, R.C.; Mahan, L.C. *Proc. Natl. Acad. Sci. U.S.A.*, **1995**, 92, 9742.
- [71] Gustafsson, J.; Arvidson, G.; Karlsson, G.; Almgren, M. *Biochim. Biophys. Acta*, **1995**, 1235, 305.
- [72] Filion, M.C.; Phillips, N.C. *Biochim. Biophys. Acta*, **1997**, 1329, 345.
- [73] Plank, C.; Mechtler, K.; Szoka, J.; Wagner, E. *Hum. Gene Ther.*, **1996**, 7, 1437.
- [74] Mahato, R.I.; Kawabata, K.; Nomura, T.; Takakura, Y.; Hashida, M. *J. Pharm. Res.*, **1995**, 84, 1267.
- [75] Ibanez, M.; Gariglio, P.; Chavez, P.; Santiago, R.; Wong, C.; Baeza, I. *Biochemistry and Cell Biology-Biochimie Et Biologie Cellulaire*, **1996**, 74, 633.
- [76] Shangguan, T.; Cabral-Lilly, D.; Purandare, U.; Godin, N.; Ahl, P.; Janoff, A.; Meers, P. *Gene Ther.*, **2000**, 7, 769.
- [77] Stuart, D.D.; Allen, T.M. *Biochim. Biophys. Acta*, **2000**, 1463, 219.
- [78] Semple, S.C.; Klimuk, S.K.; Harasyn, T.O.; Dos Santos, N.; Ansell, S.M.; Wong, K.F.; Maurer, N.; Stark, H.; Cullis, P.R.; Hope, M.J.; Scherrer, P. *Biochim. Biophys. Acta*, **2001**, 1510, 152.
- [79] Bailey, A.L.; Sullivan, S.M. *Biochim. Biophys. Acta*, **2000**, 1468, 239.
- [80] Kikuchi, H.; Suzuki, N.; Ebihara, K.; Morita, H.; Ishii, Y.; Kikuchi, A.; Sugaya, S.; Serikawa, T.; Tanaka, K. *J. Control. Release*, **1999**, 62, 269.
- [81] Tabor, C.W.; Tabor, H. *Annu. Rev. Biochem.*, **1984**, 53, 749.
- [82] Ames, B.N.; Dubin, D.T. *J. Biol. Chem.*, **1960**, 253, 769.
- [83] Pelta, J.; Livolant, F.; Sikorav, J.L. *J. Biol. Chem.*, **1996**, 271, 5656.
- [84] Pelta, J.; Durand, D.; Doucet, J.; Livolant, F. *Biophys. J.*, **1996**, 71, 48.
- [85] Raspaud, E.; delaCruz, M.O.; Sikorav, J.L.; Livolant, F. *Biophys. J.*, **1998**, 74, 381.
- [86] Fang, Y.; Hoh, J.H. *J. Am. Chem. Soc.*, **1998**, 120, 8903.
- [87] Raghavachari, N.; Fahl, W.E. *J. Pharm. Sci.*, **2002**, 91, 615.
- [88] Kisak, E.T.; Coldren, B.; Zasadzinski, J.A. *Langmuir*, **2002**, 18, 284.
- [89] Lasic, D.D. *Angew. Chem., Int. Ed.*, **1994**, 33, 1685.
- [90] Silvander, M.; Johnsson, M.; Edwards, K. *Chem. Phys. Lipids*, **1998**, 97, 15.
- [91] Mui, B.L.S.; Cullis, P.R.; Evans, E.A.; Madden, T.D. *Biophys. J.*, **1993**, 64, 443.
- [92] Webb, M.S.; Wheeler, J.J.; Bally, M.B.; Mayer, L.D. *Biochim. Biophys. Acta*, **1995**, 1238, 147.

- [93] Paula, S.; Volkov, A.G.; Deamer, D.W. *Biophys. J.*, **1998**, *74*, 319.
- [94] Semple, S.C.; Chonn, A.; Cullis, P.R. *Adv. Drug Delivery Rev.*, **1998**, *32*, 3.
- [95] Mayer, L.D.; Reamer, J.; Bally, M.B. *J. Pharm. Sci.*, **1999**, *88*, 96.
- [96] Mayer, L.D.; Tai, L.C.L.; Ko, D.S.C.; Masin, D.; Ginsberg, R.S.; Cullis, P.R.; Bally, M.B. *Cancer Res.*, **1989**, *49*, 5922.
- [97] Waterhouse, D.N.; Dos Santos, N.; Mayer, L.D.; Bally, M.B. *Pharm. Res.*, **2001**, *18*, 1331.
- [98] Johnson, S.M.; Bangham, A.D. *Biochim. Biophys. Acta*, **1969**, *193*, 82.
- [99] Hamilton, R.T.; Kaler, E.W. *J. Phys. Chem.*, **1990**, *94*, 2560.
- [100] Parsegian, A. *Nature*, **1969**, *221*, 844.
- [101] Dilger, J.P.; McLaughlin, S.G.A.; McIntosh, T.J.; Simon, S.A. *Science*, **1979**, *206*, 1196.
- [102] Evans, D.F.; Wennerstrom, H. *The Colloidal Domain*, VCH Publishers: New York, **1994**.
- [103] Cussler E.L. *Diffusion: Mass Transfer in Fluid Systems*, Cambridge University Press: Cambridge, **1997**.
- [104] Yatvin, M.B.; Weinstein, J.N.; Dennis, W.H.; Blumenthal, R. *Science*, **1978**, *202*, 1290.
- [105] Nagle, J.F.; Scott, H.L. *Biochim. Biophys. Acta*, **1978**, *513*, 236.
- [106] Helfrich, W. *Z. Naturforsch.*, **1973**, *28c*, 693.
- [107] Evans, E.; Rawicz, W. *Phys. Rev. Lett.*, **1990**, *64*, 2094.
- [108] Rawicz, W.; Olbrich, K.C.; McIntosh, T.; Needham, D.; Evans, E. *Biophys. J.*, **2000**, *79*, 328.
- [109] Jung, H.T.; Coldren, B.; Zasadzinski, J.A.; Iampietro, D.; Kaler, E.W. *Proc. Natl. Acad. Sci. U.S.A.*, **2001**, *98*, 1353.
- [110] Jung, H.T.; Lee, S.Y.; Coldren, B.; Zasadzinski, J.A.; Kaler, E.W. *Proc. Natl. Acad. Sci. U.S.A.*, **2002**, *99*, 15318.
- [111] Safran, S.A.; Pincus, P.; Andelman, D. *Science*, **1990**, *248*, 354.
- [112] Grandbois, M.; Clausen-Schaumann, H.; Gaub, H. *Biophys. J.*, **1998**, *74*, 2398.
- [113] Davidsen, J.; Jorgensen, K.; Andresen, T.L.; Mouritsen, O.G. *Biochim. Biophys. Acta*, **2003**, *1609*, 95.
- [114] Berg, O.G.; Gelb, M.H.; Tsai, M.-D.; Jain, M.L. *Chem. Rev.*, **2001**, *101*, 2613.